Resolving the Hadronic Accelerator IC 443:

A Joint Study with Fermi-LAT and VERITAS

J.W. Hewitt (Univ. of North Florida)
E.A. Hays, J. Schmid, H. Tajima,
on behalf of the *Fermi* LAT
and VERITAS collaborations

6th Fermi Symposium, Nov. 11, 2015

IC 443: Interacting with a Multi-Phase ISM

- Evolved (radiative) SNR interacting with a molecular cloud

WISE 3-color IR image of shocked dust

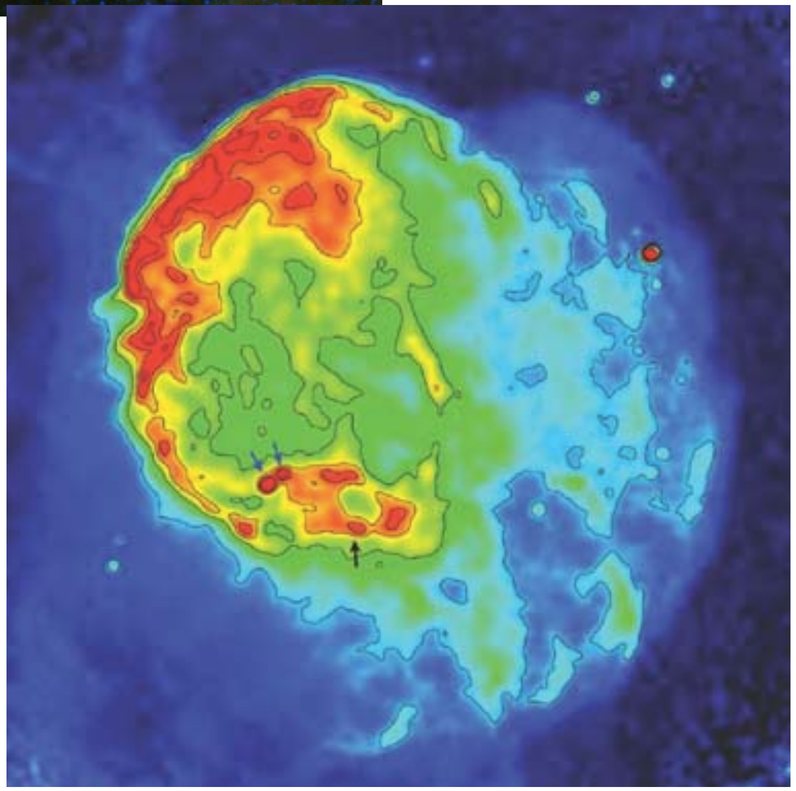

Radio 20cm

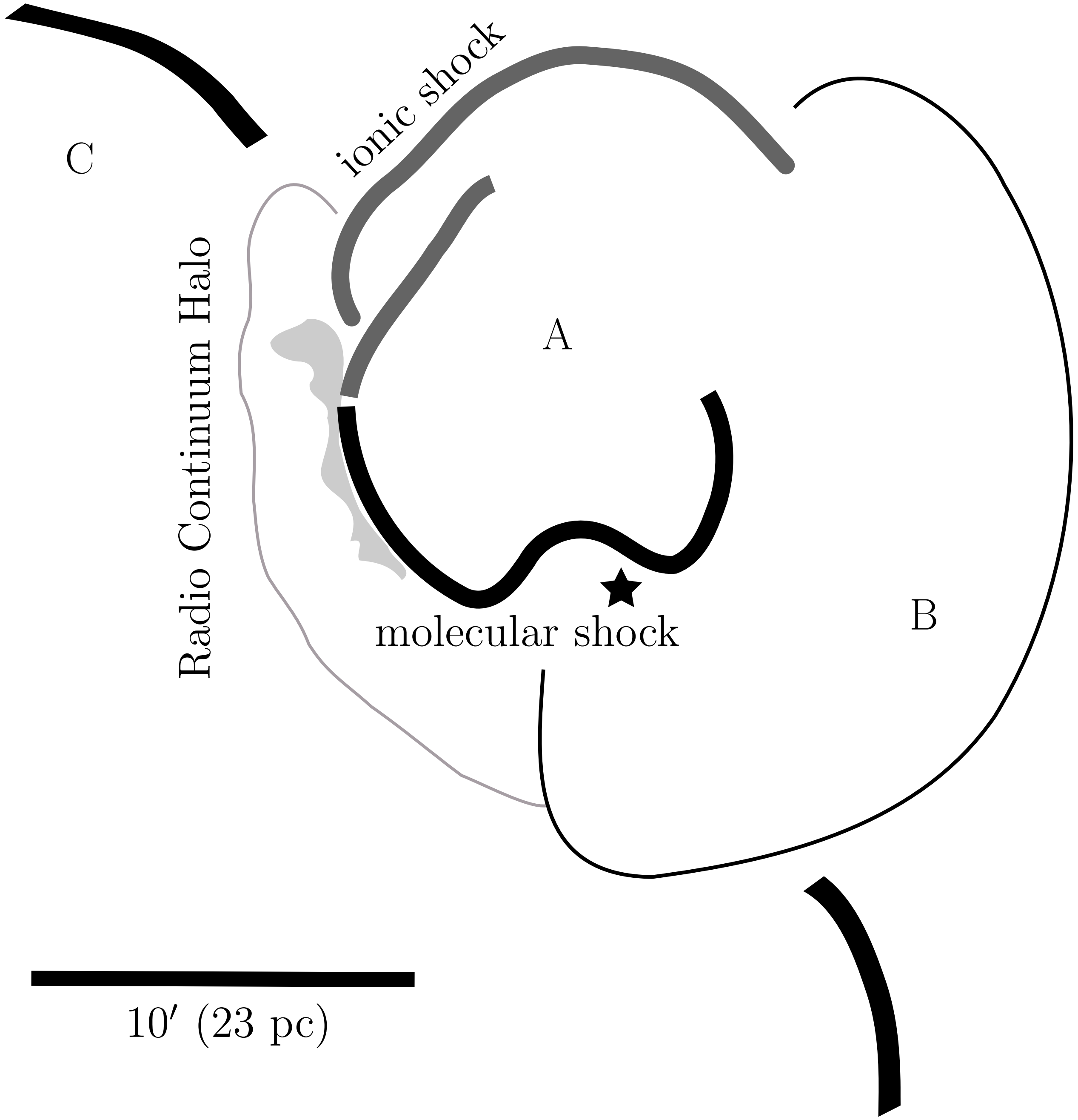

Schematic of IC 443 from Lee, et al. (2008)

IC 443: Prominent γ-ray Supernova Remnant

- GeV γ rays detected by EGRET in 90's. TeV γ rays detected by MAGIC, VERITAS→
- Spatially extended in GeV/TeV γ rays
- Later AGILE, *Fermi*-LAT detect π^0 bump (e.g. Abdo, et al. 2012) ↓

(Note: Images always oriented in J2000)

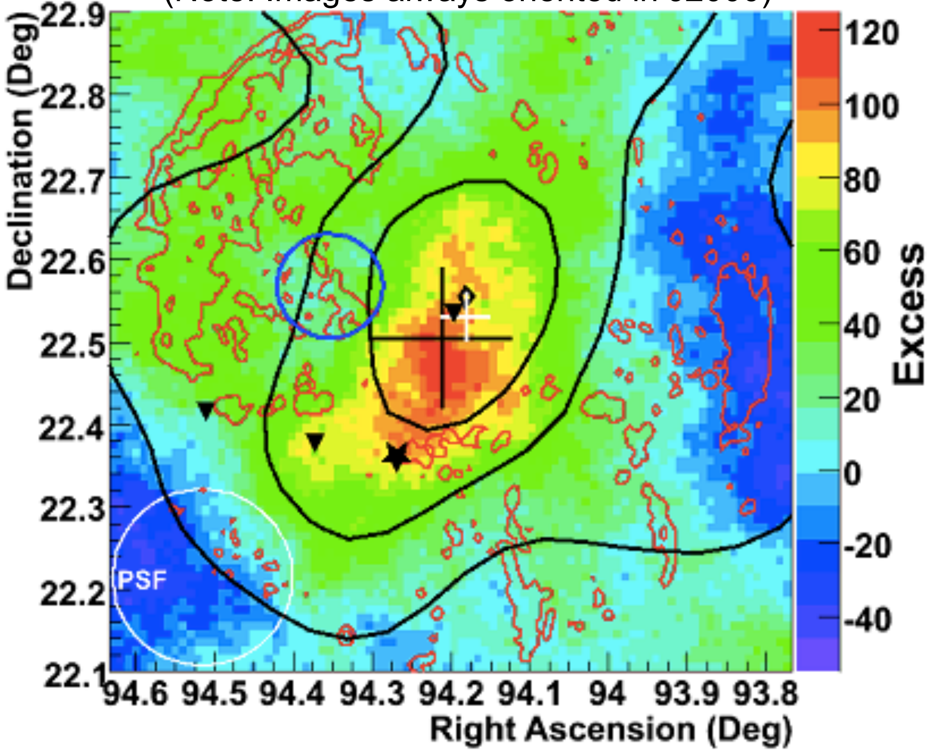

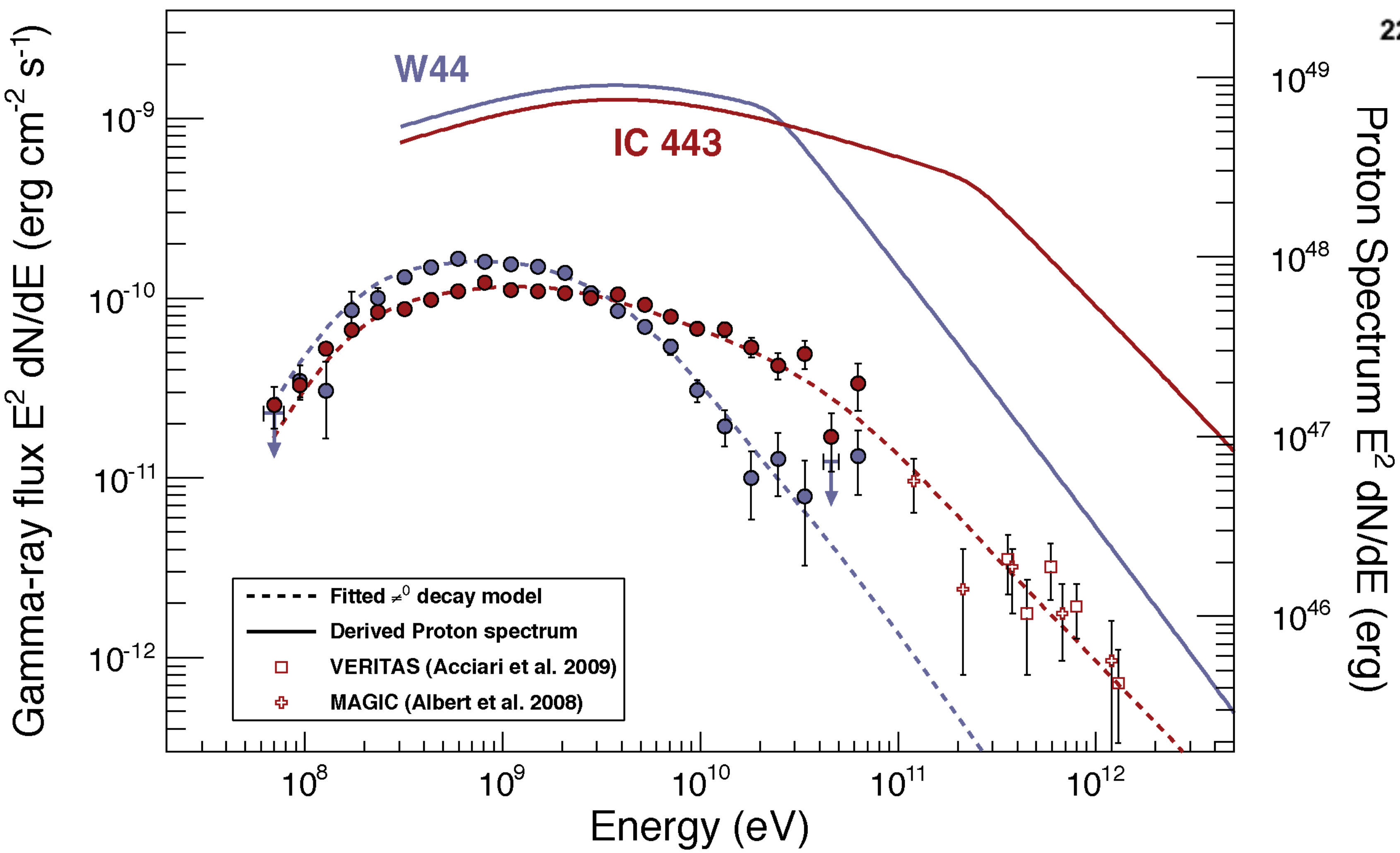

Our Improving γ ray Views

***Fermi* LAT** 2010: 13 mos. P6V3 data

VERITAS 2007: 38hrs

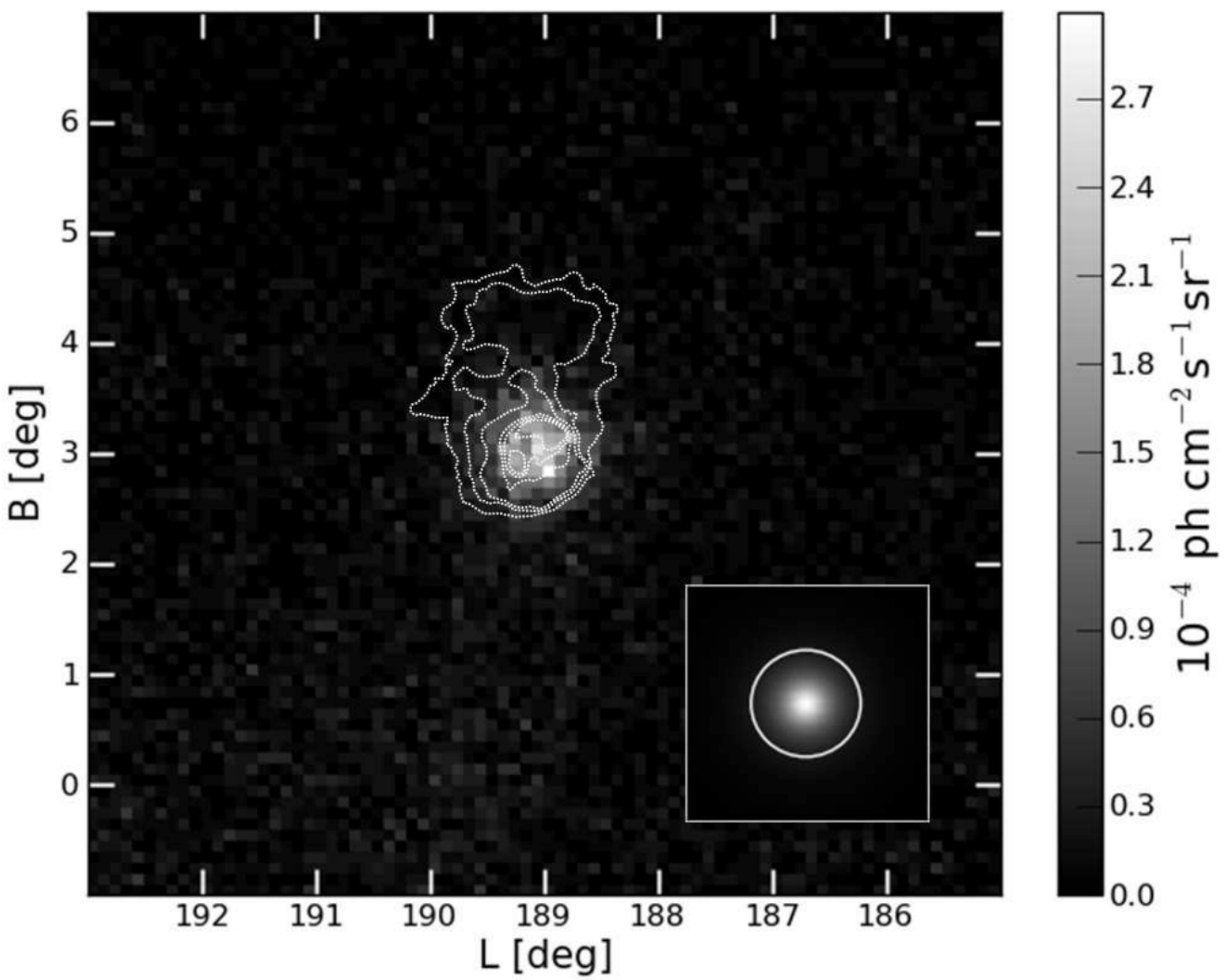

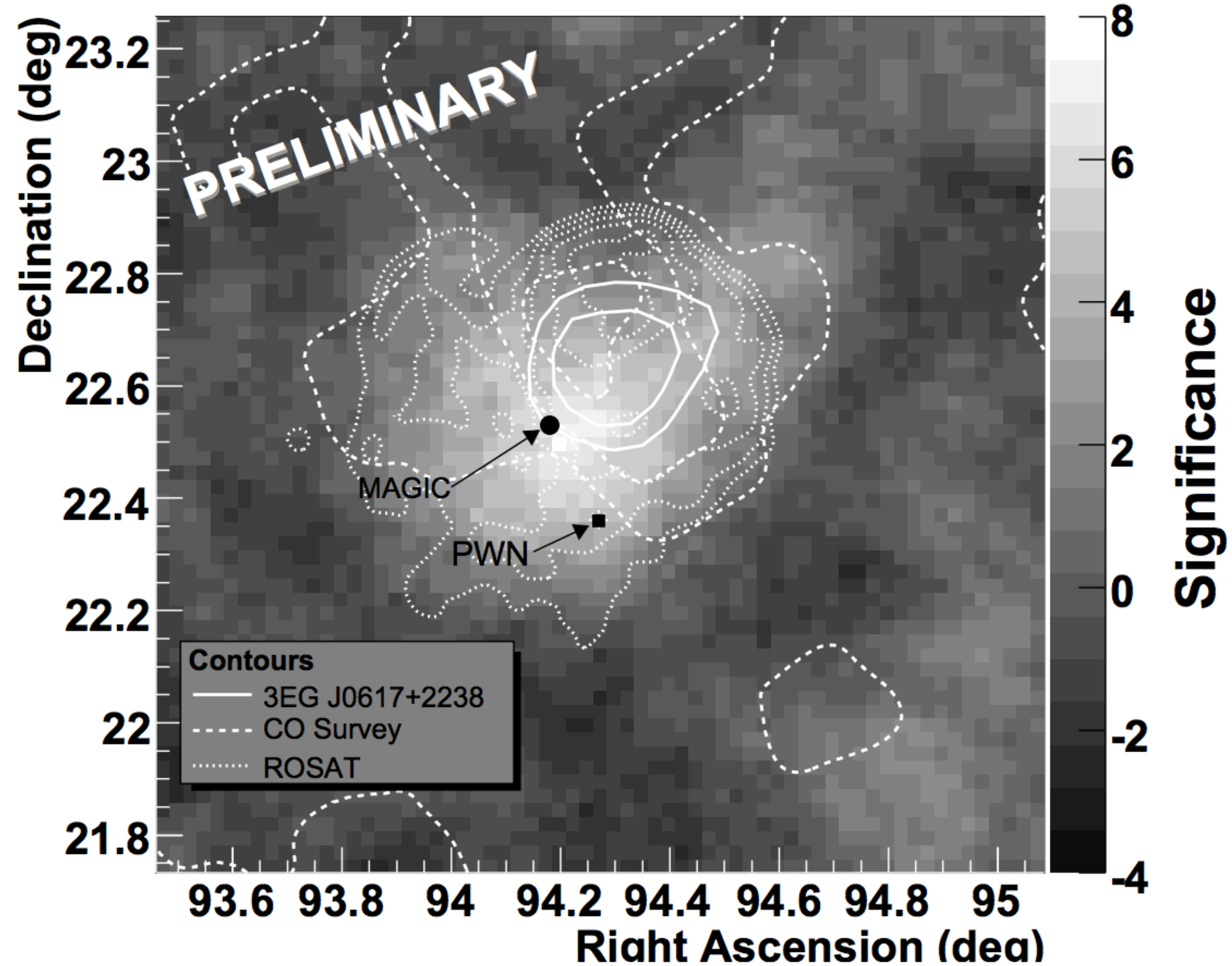

Our Improving γ ray Views

Fermi **LAT** 2010: 13 mos. P6V3 data → 2015: 83 mos. Pass 8 data

VERITAS 2007: 38hrs → 2015: 178hrs + PMT upgrade, T1 move

IC 443 is resolved as a γ-ray shell SNR

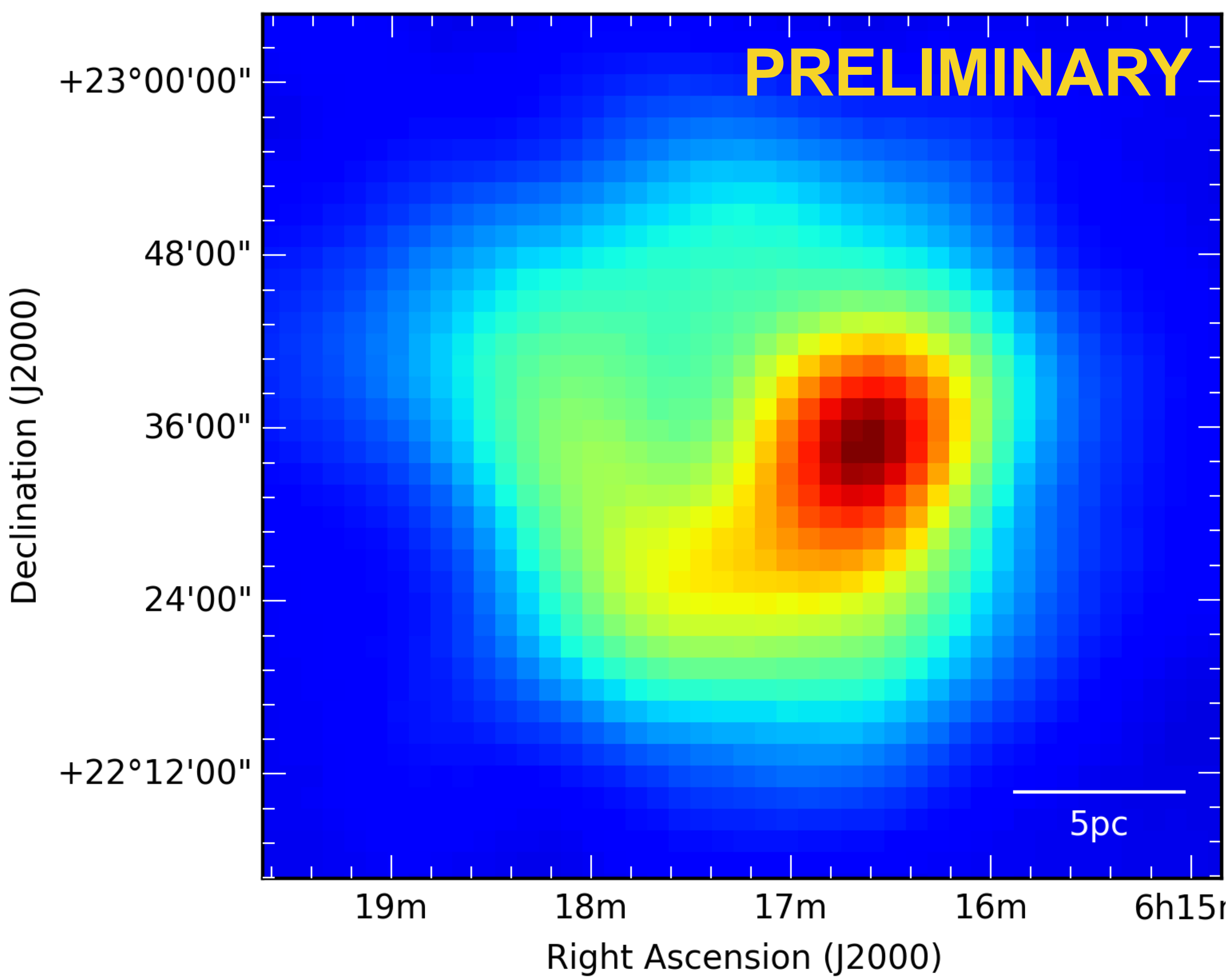

Counts Map >5 GeV (PSF23)

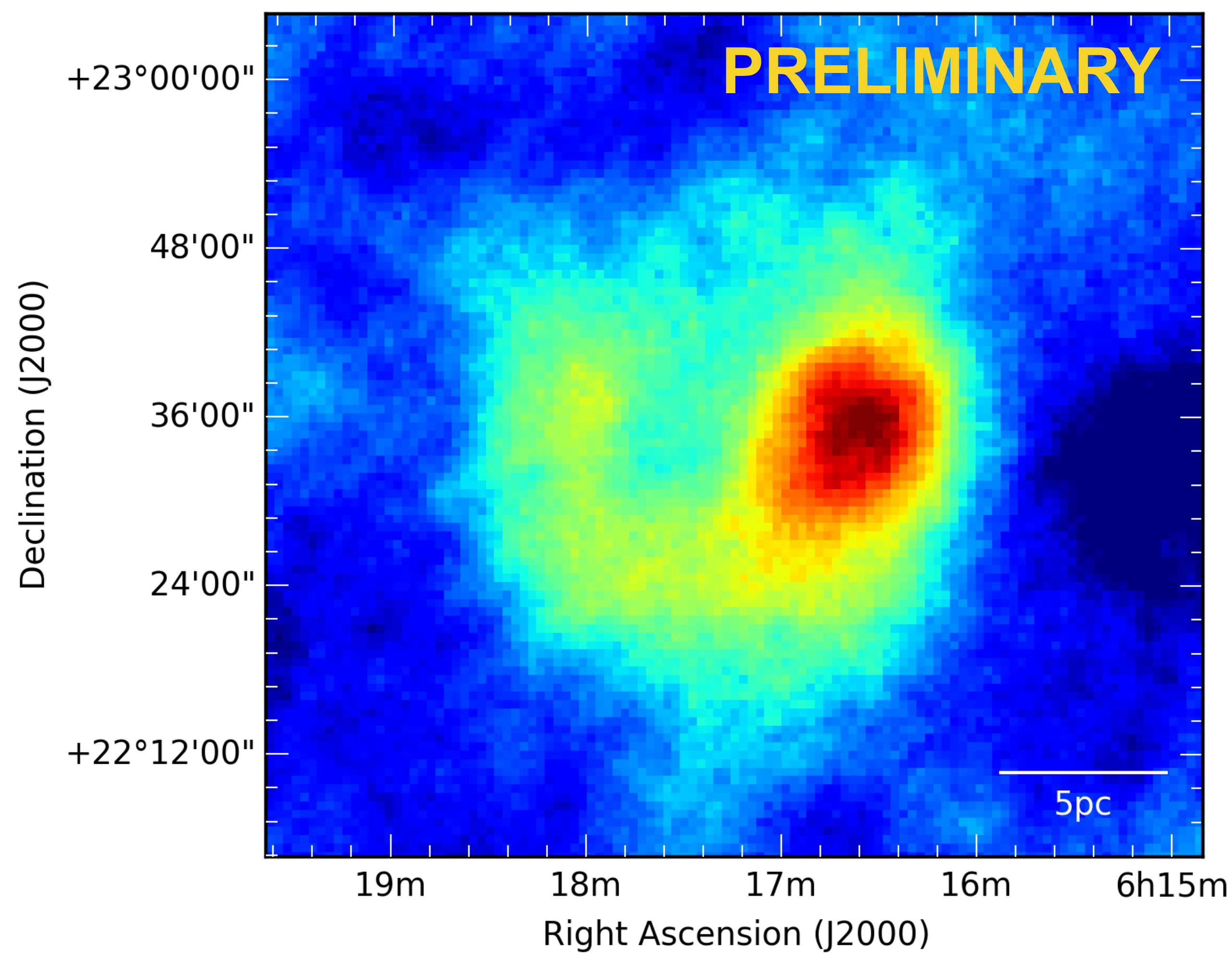

Significance Map

Utilizing PSF Event Types in Pass 8

LAT morphology compared to **TeV** - VERITAS contours at 3,6,9,12 σ

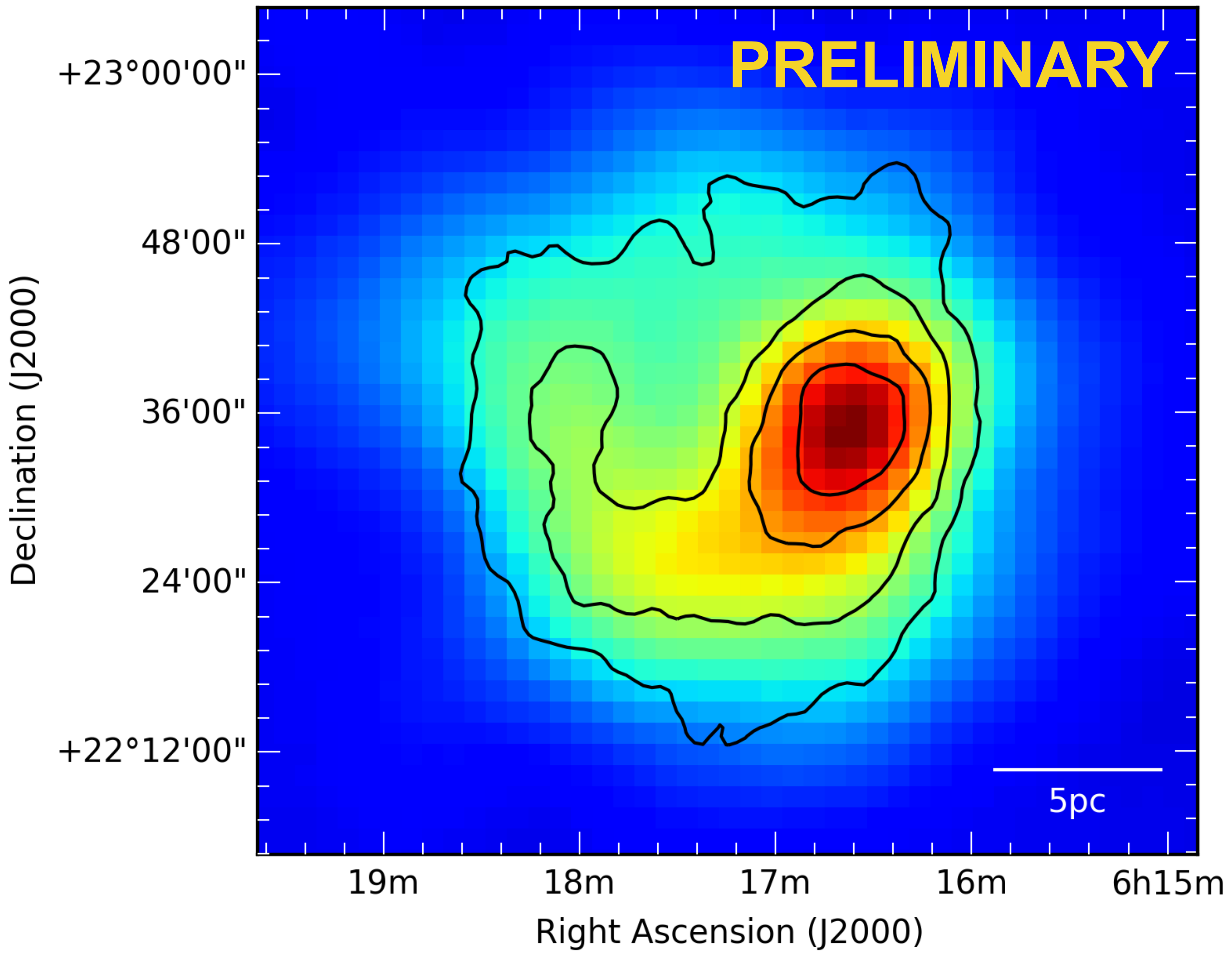

Counts Map >5 GeV (PSF23)

See Sajan Kumar's poster (SNR 5) for VERITAS details

Utilizing PSF Event Types in Pass 8

LAT morphology compared to TeV, **radio** - 327 MHz continuum

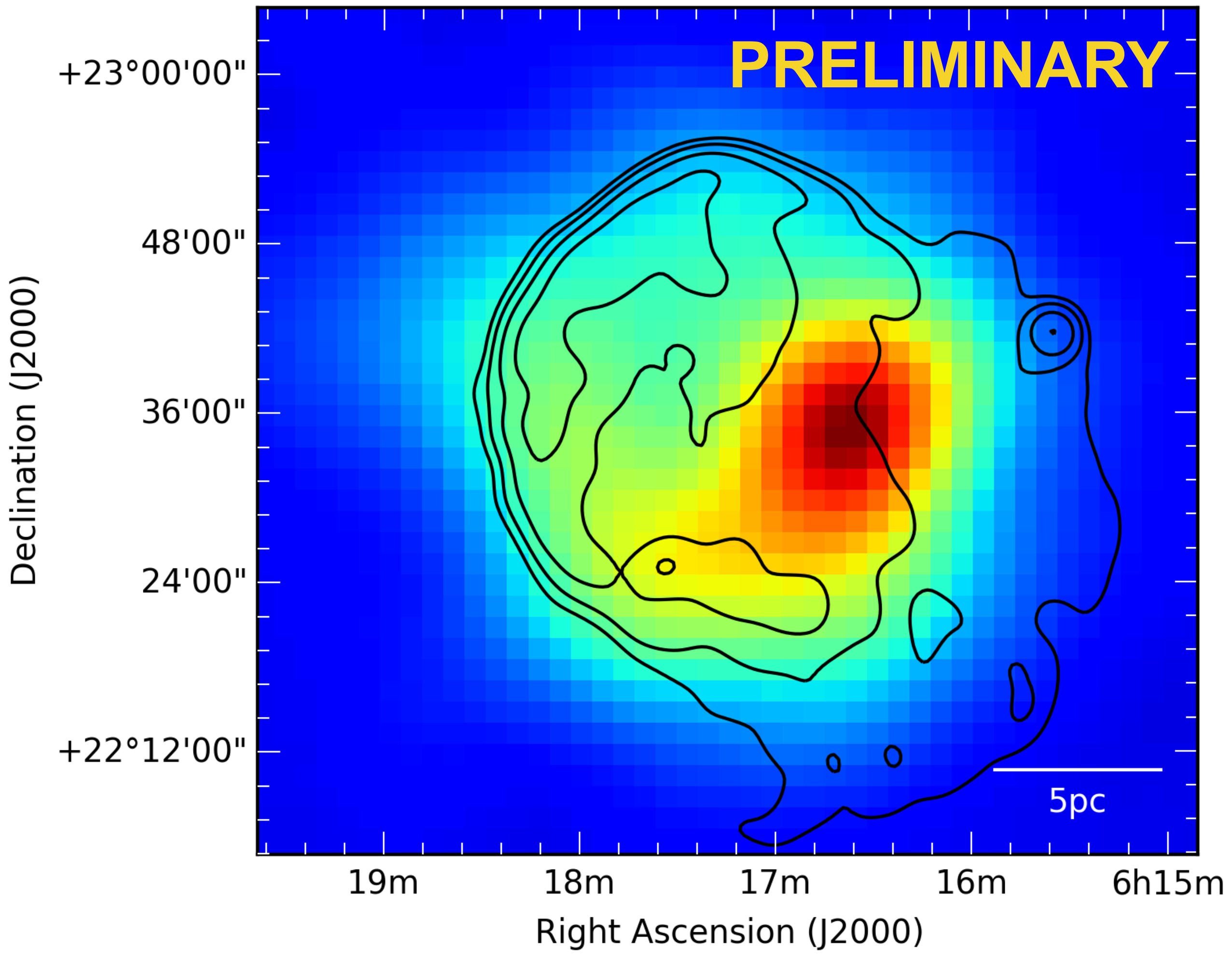

Counts Map >5 GeV (PSF23)

Utilizing PSF Event Types in Pass 8

LAT morphology compared to TeV, ~~radio~~, **ambient CO**

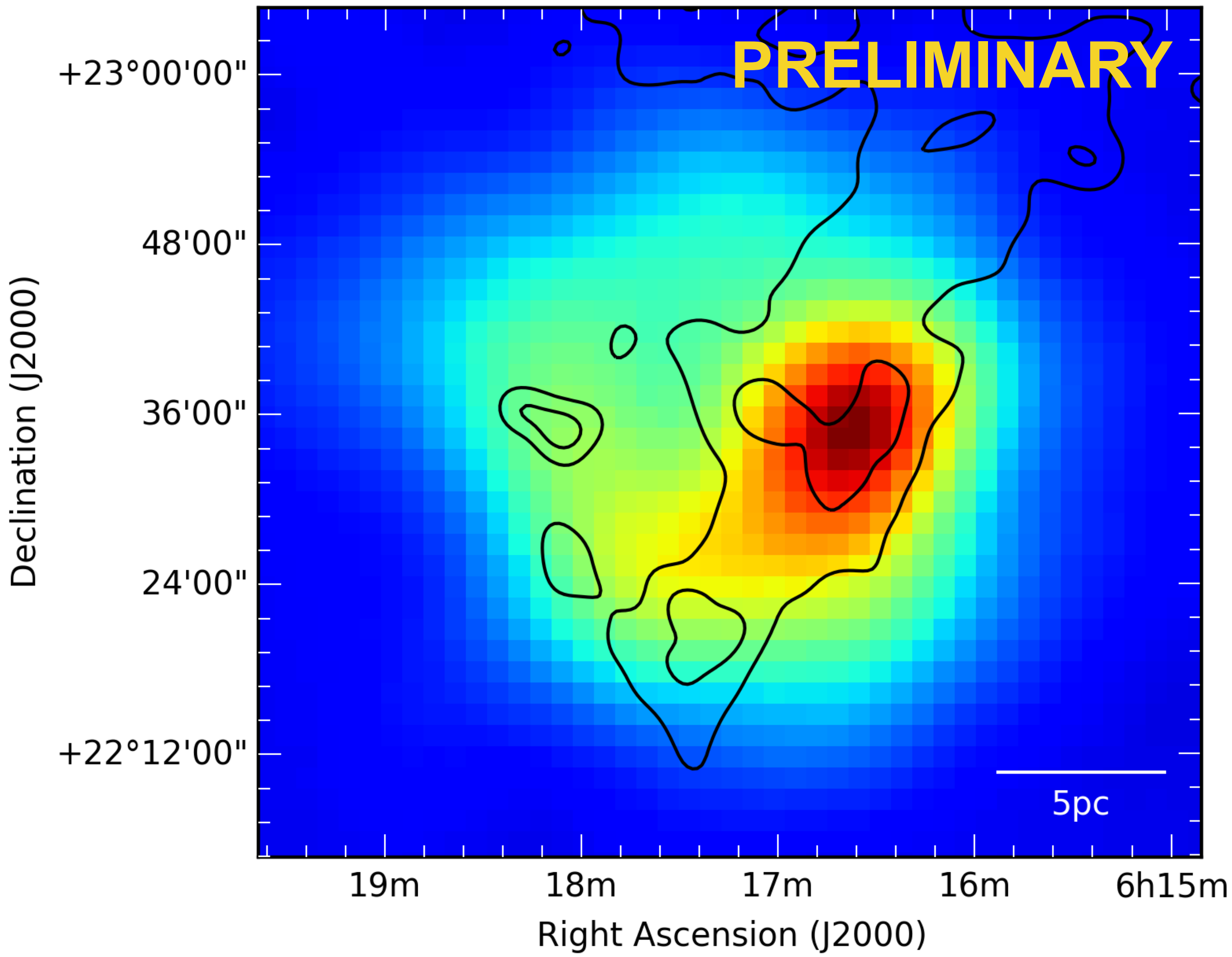

Counts Map >5 GeV (PSF23)

Utilizing PSF Event Types in Pass 8

LAT morphology compared to TeV, ~~radio~~, ~~ambient CO~~, **shocked HCO+**

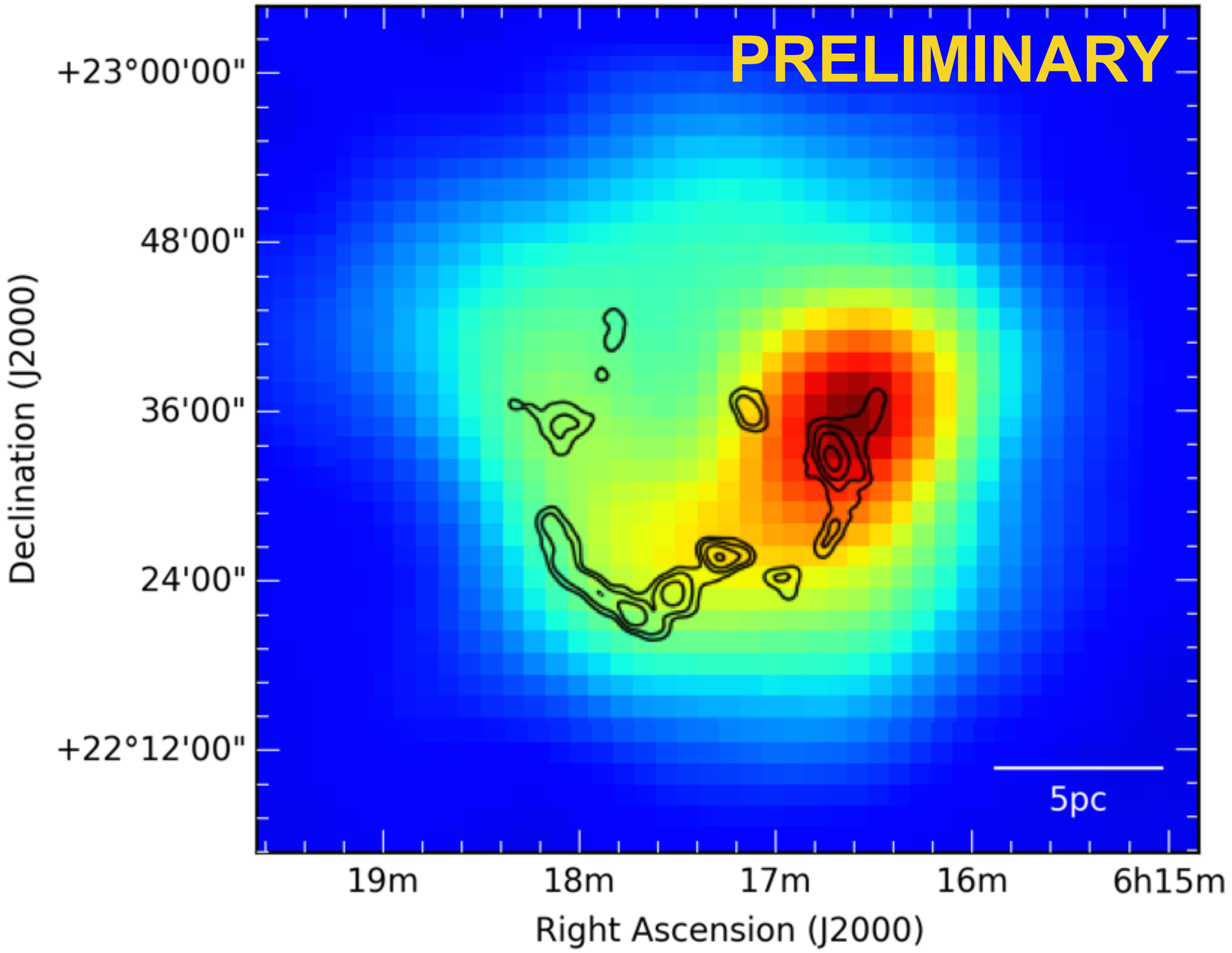

Counts Map >5 GeV (PSF23)

Utilizing PSF Event Types in Pass 8

- Multi-wavelength comparison shows the GeV/TeV γ rays match the distribution of *shocked* gas in IC 443

LAT morphology compared to TeV, ~~radio~~, ~~ambient CO~~, **shocked HCO+**

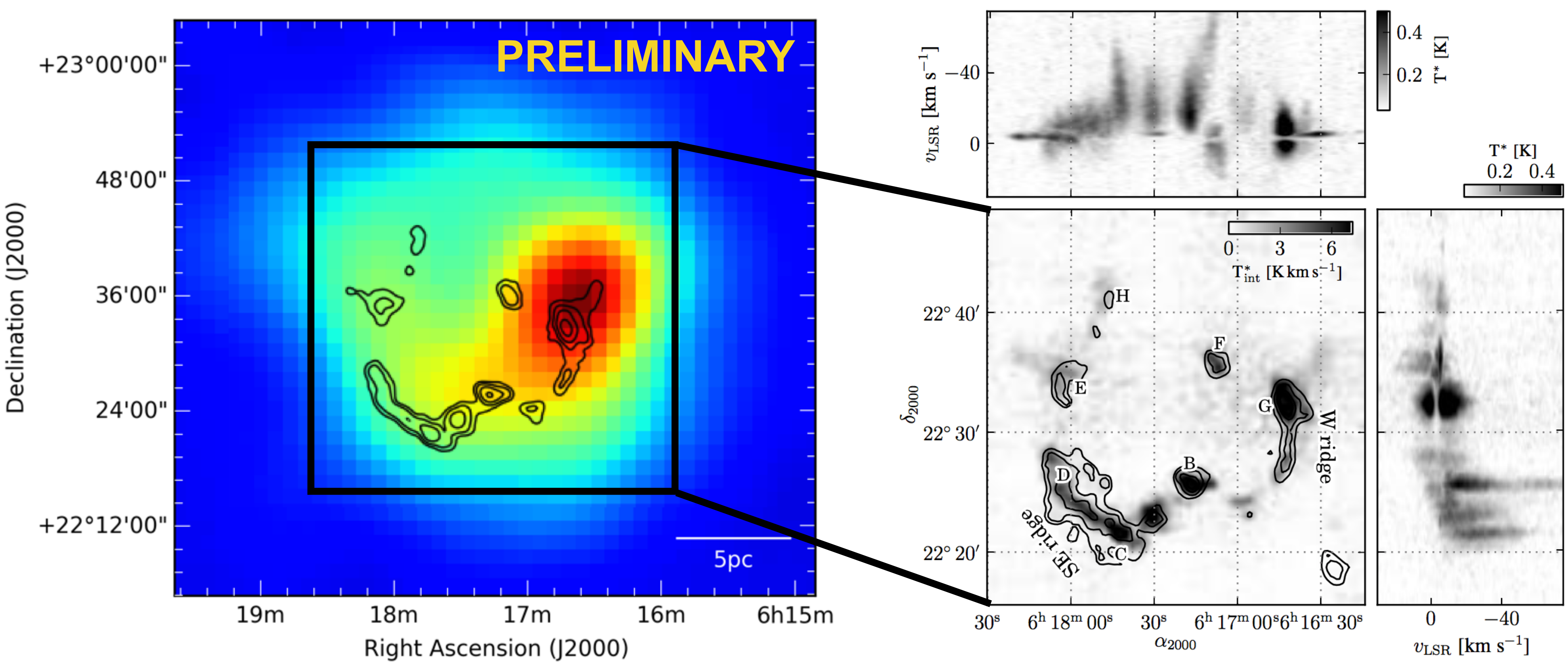

Counts Map >5 GeV (PSF23)

~10^4 M_{sun} of shocked gas along southern ridge (Lee, et al. 2008)

Utilizing PSF Event Types in Pass 8

- Multi-wavelength comparison shows the GeV/TeV γ rays match the distribution of *shocked* gas in IC 443

LAT morphology compared to TeV, ~~radio~~, ~~ambient CO~~, shocked HCO+

shocked atomic gas in North?

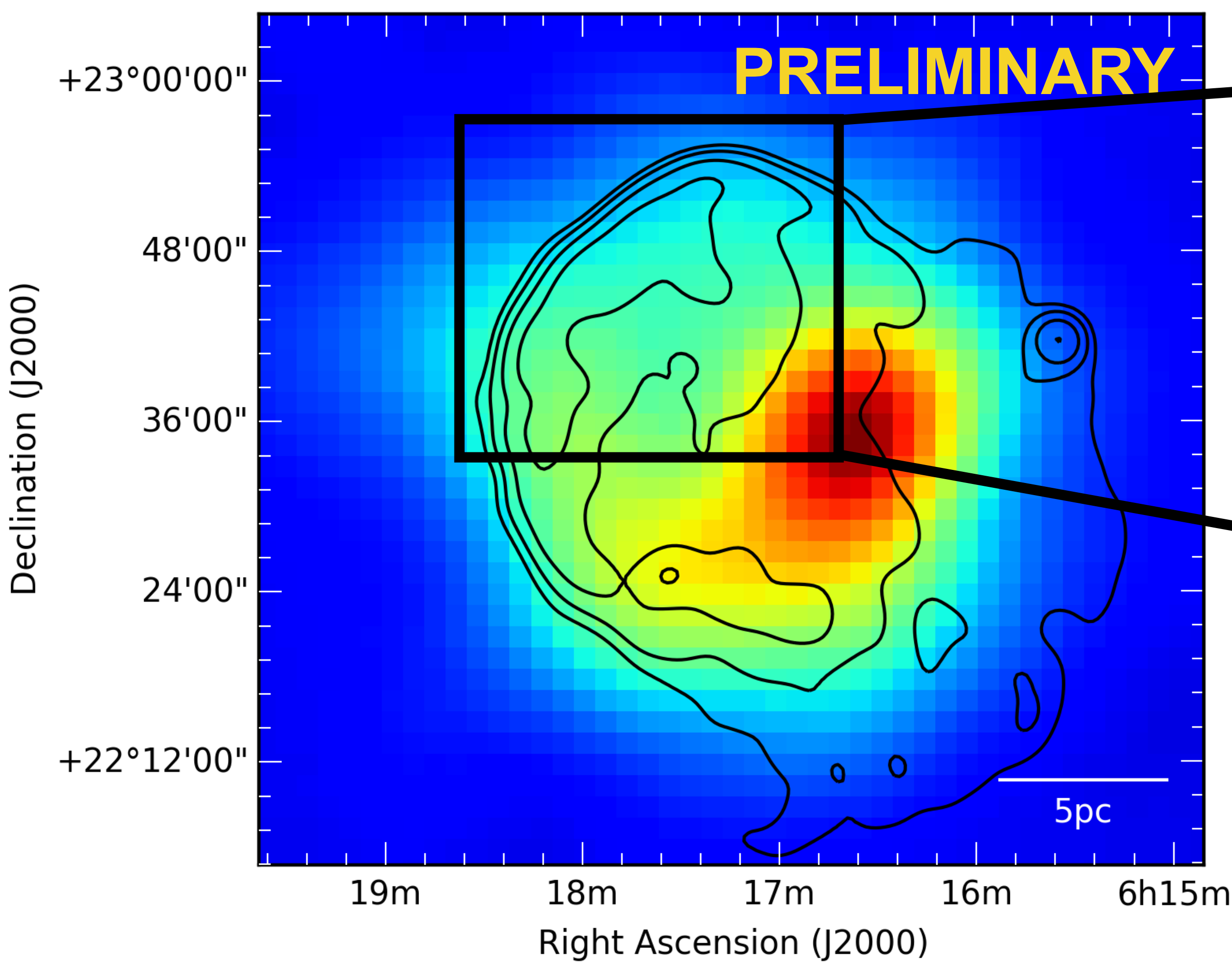

Counts Map >5 GeV (PSF23)

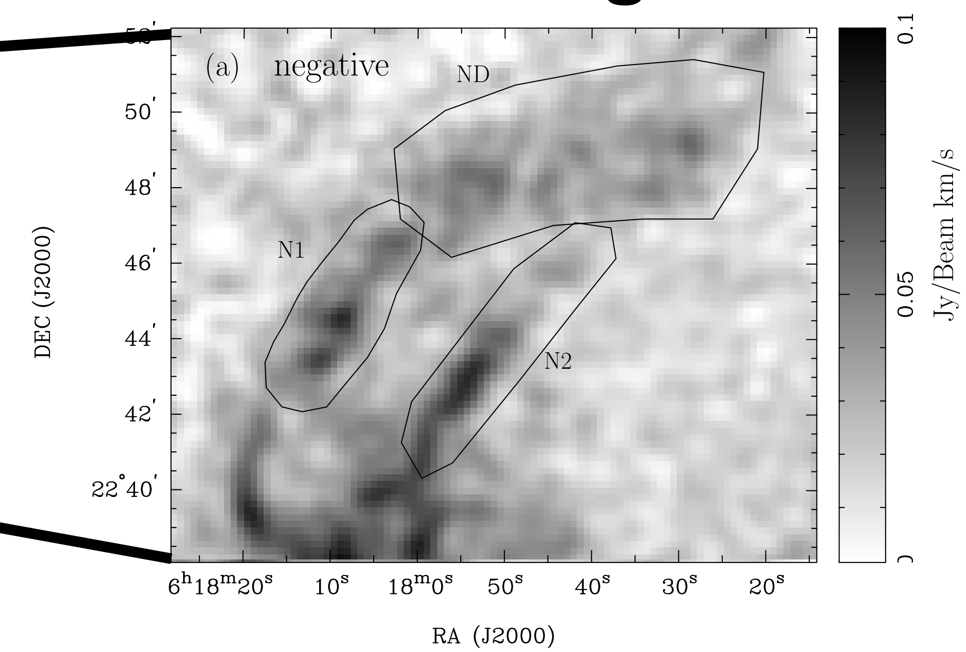

HI absorption → 40±4 M_{sun} (Castelletti, et al. 2011)

H^+ gas has n_e=10-1000 cm^{-3} (Rho, et al. 2001)

Sharper LAT Imaging

- Lucy-Richardson deconvolution with wavelet denoising enhances spatial structures (as done previously with W44; Abdo et al. 2010)

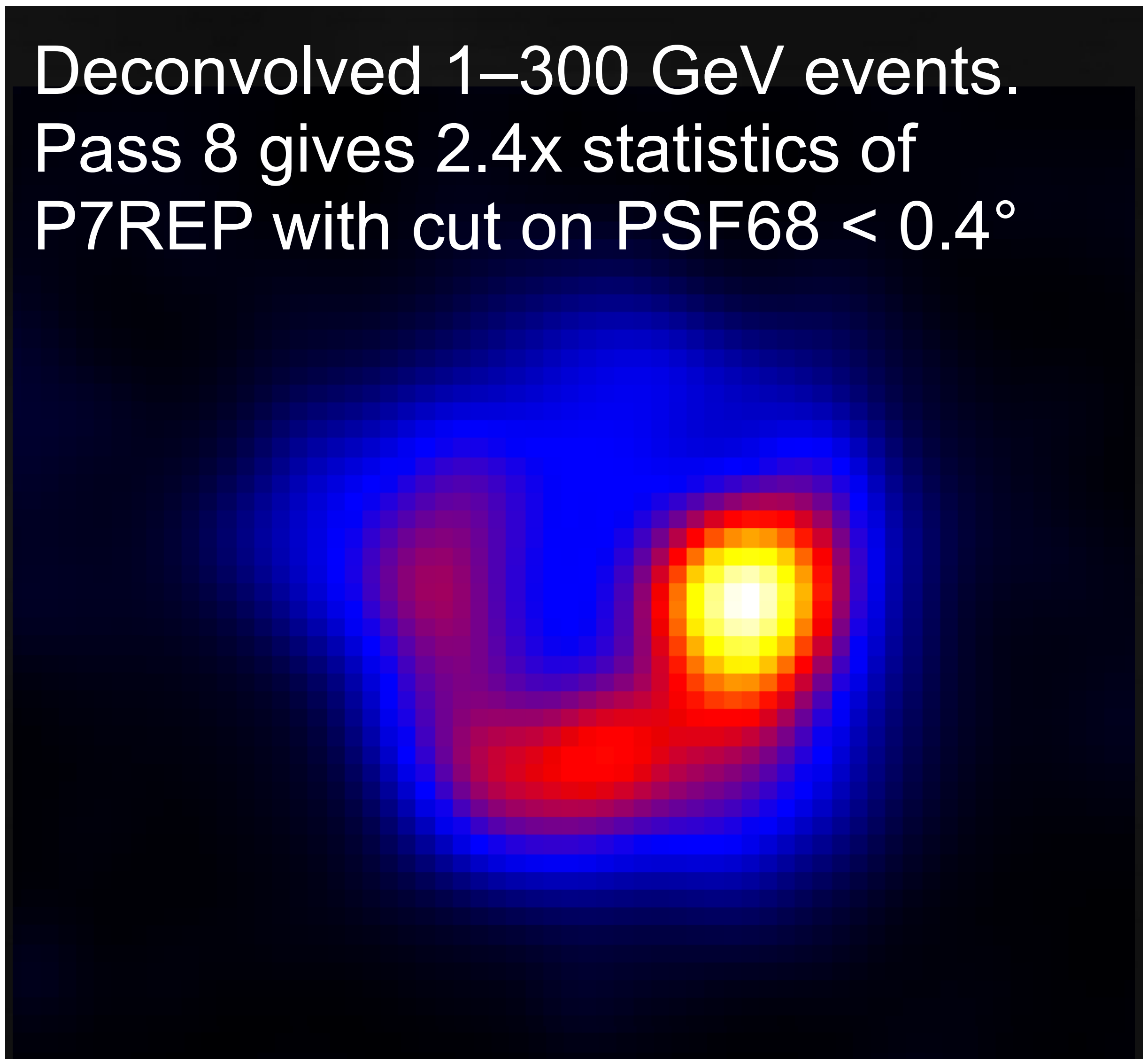

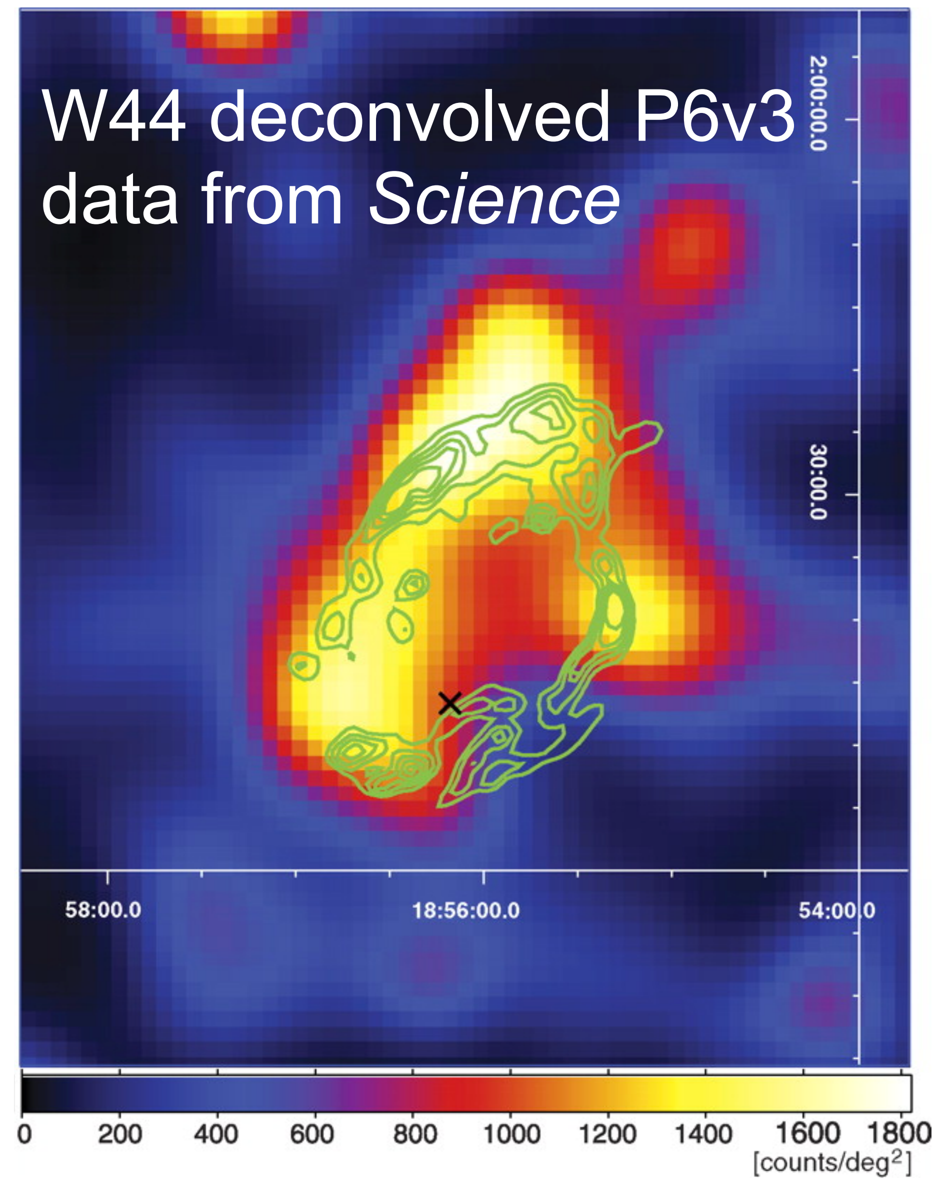

- Deconvolved LAT image is used as an extended spatial template to isolate different emission regions see arXiv:0705.1362

Sharper LAT Imaging

- Lucy-Richardson deconvolution with wavelet denoising enhances spatial structures (as done previously with W44; Abdo et al. 2010)

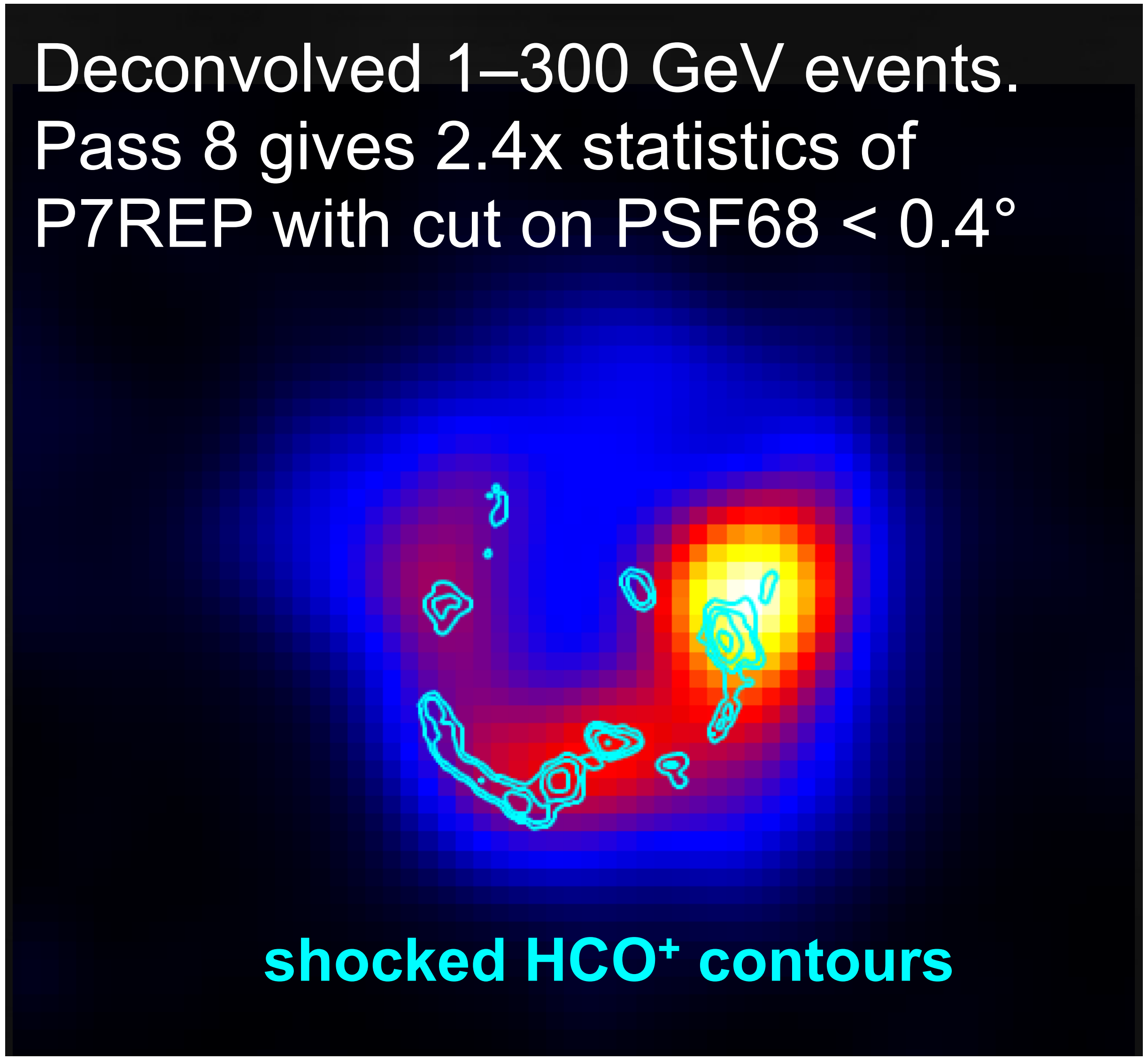

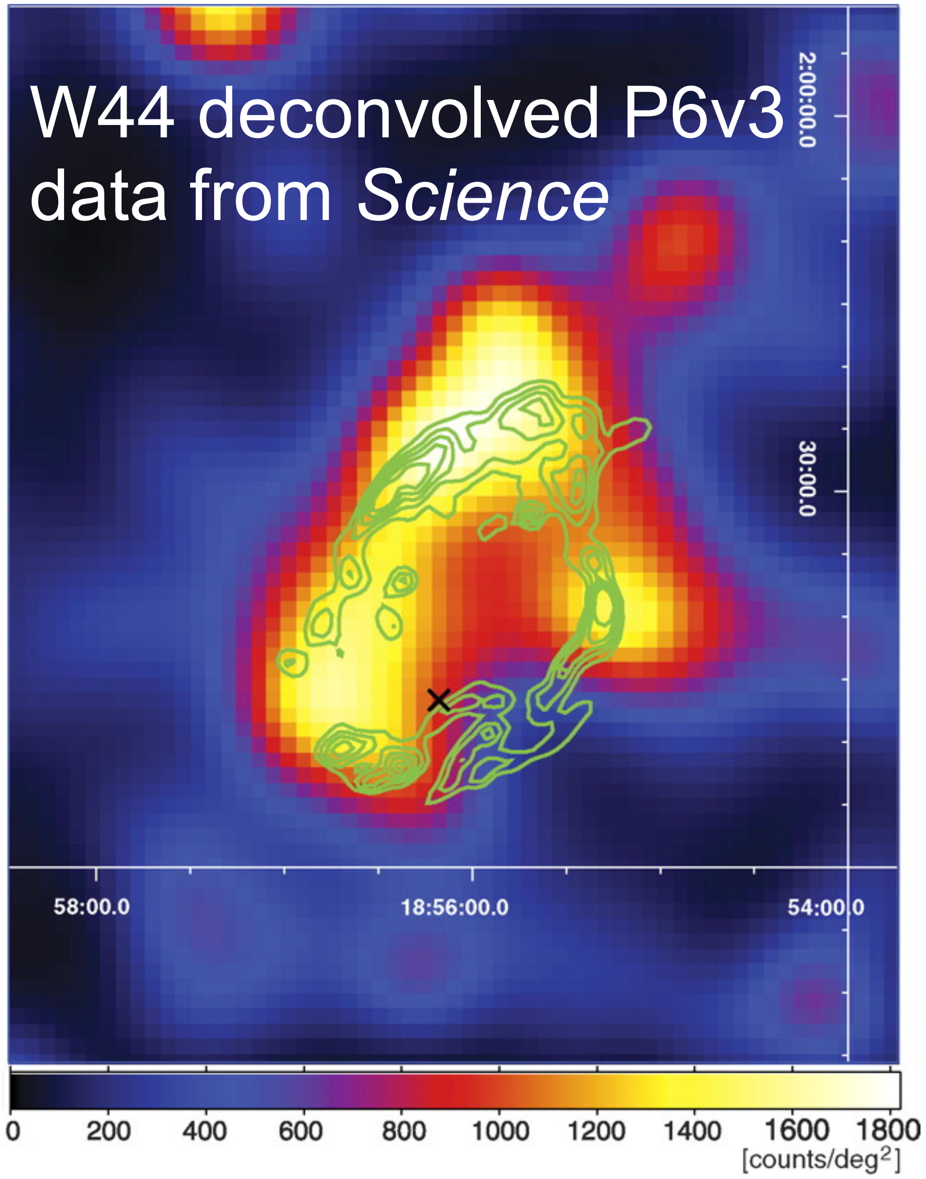

- Deconvolved LAT image is used as an extended spatial template to isolate different emission regions see arXiv:0705.1362

Exploring 4 Distinct Regions

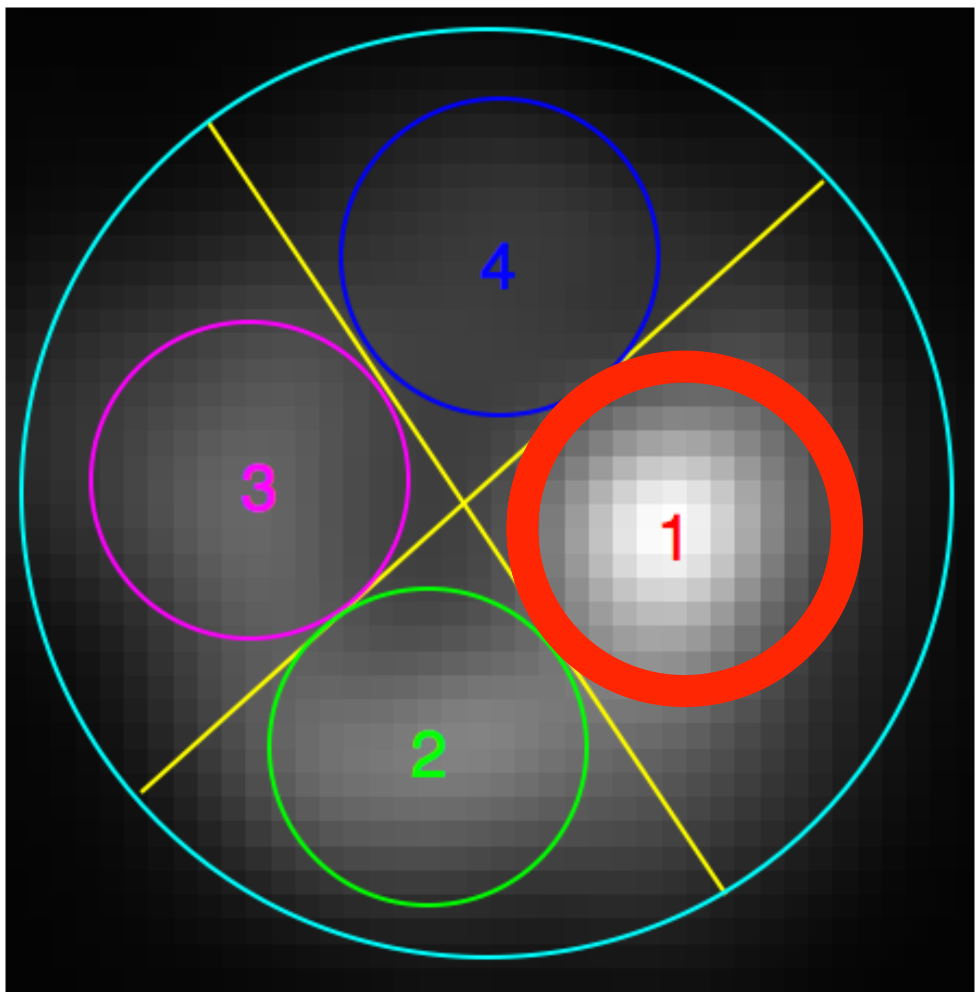

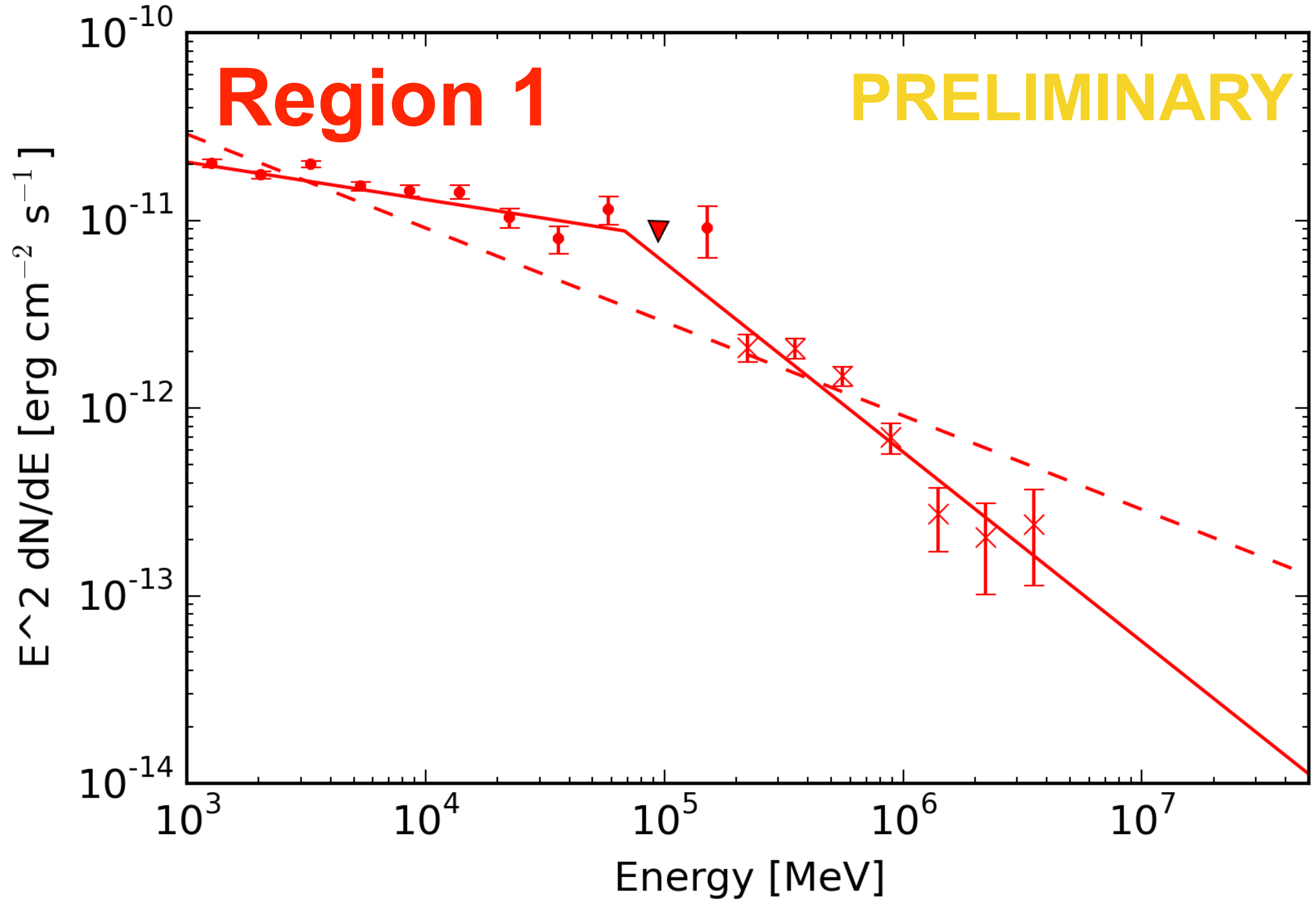

Extract spectra from distinct regions using 4 spatial templates for LAT / circular apertures for VERITAS

Exploring 4 Distinct Regions

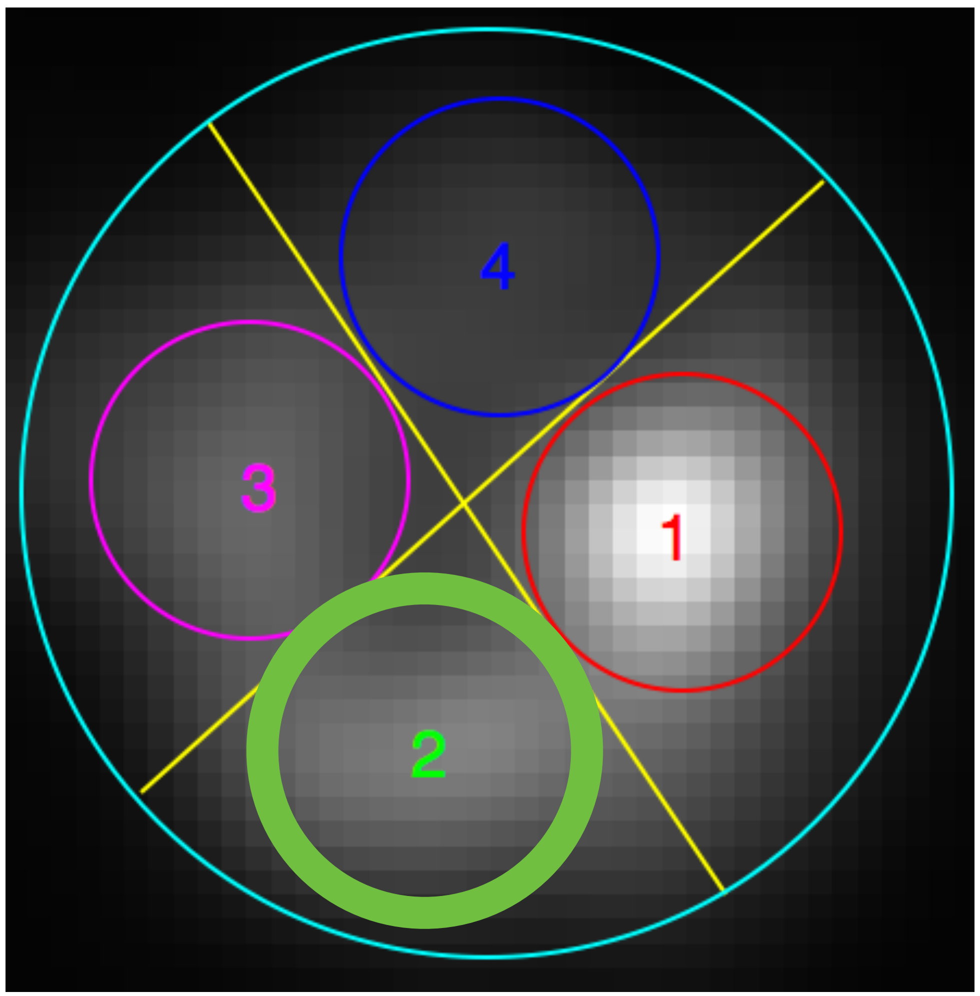

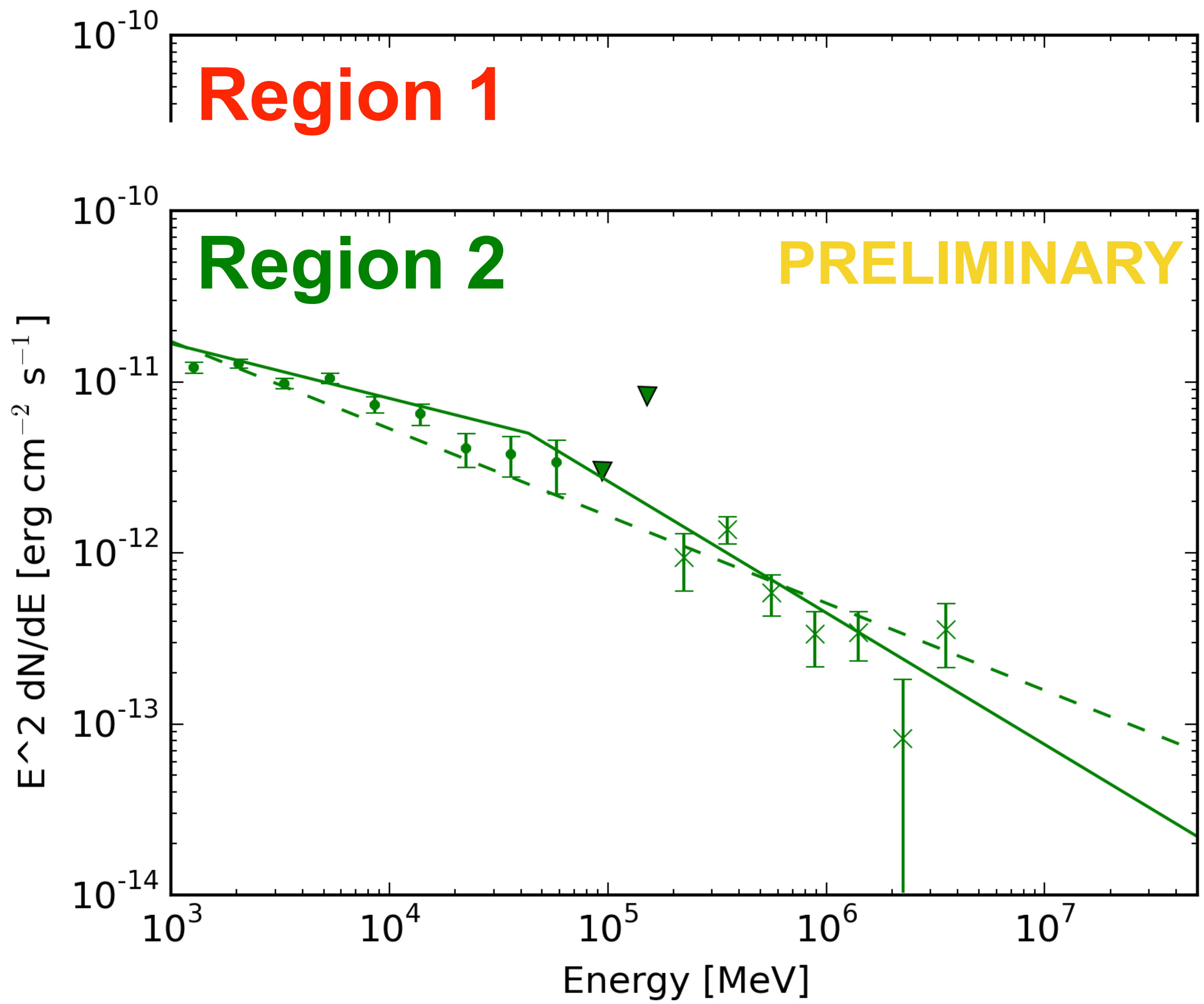

Exploring 4 Distinct Regions

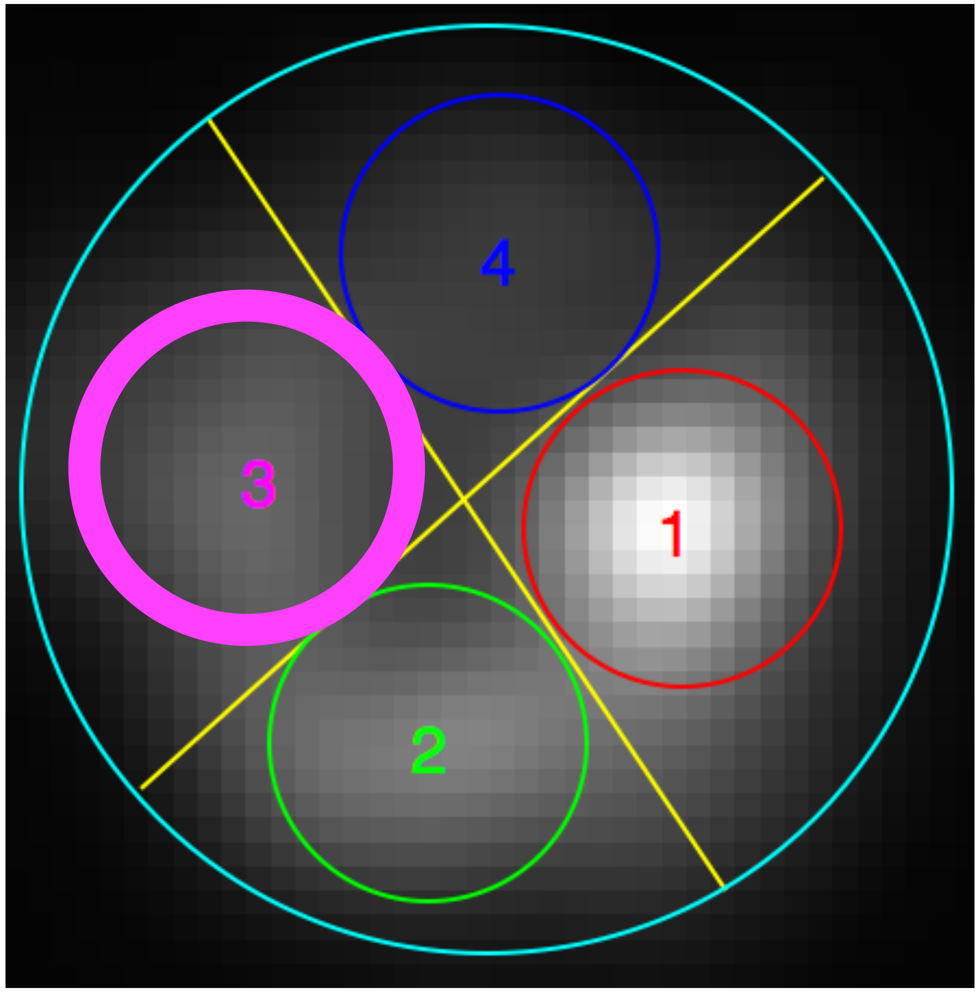

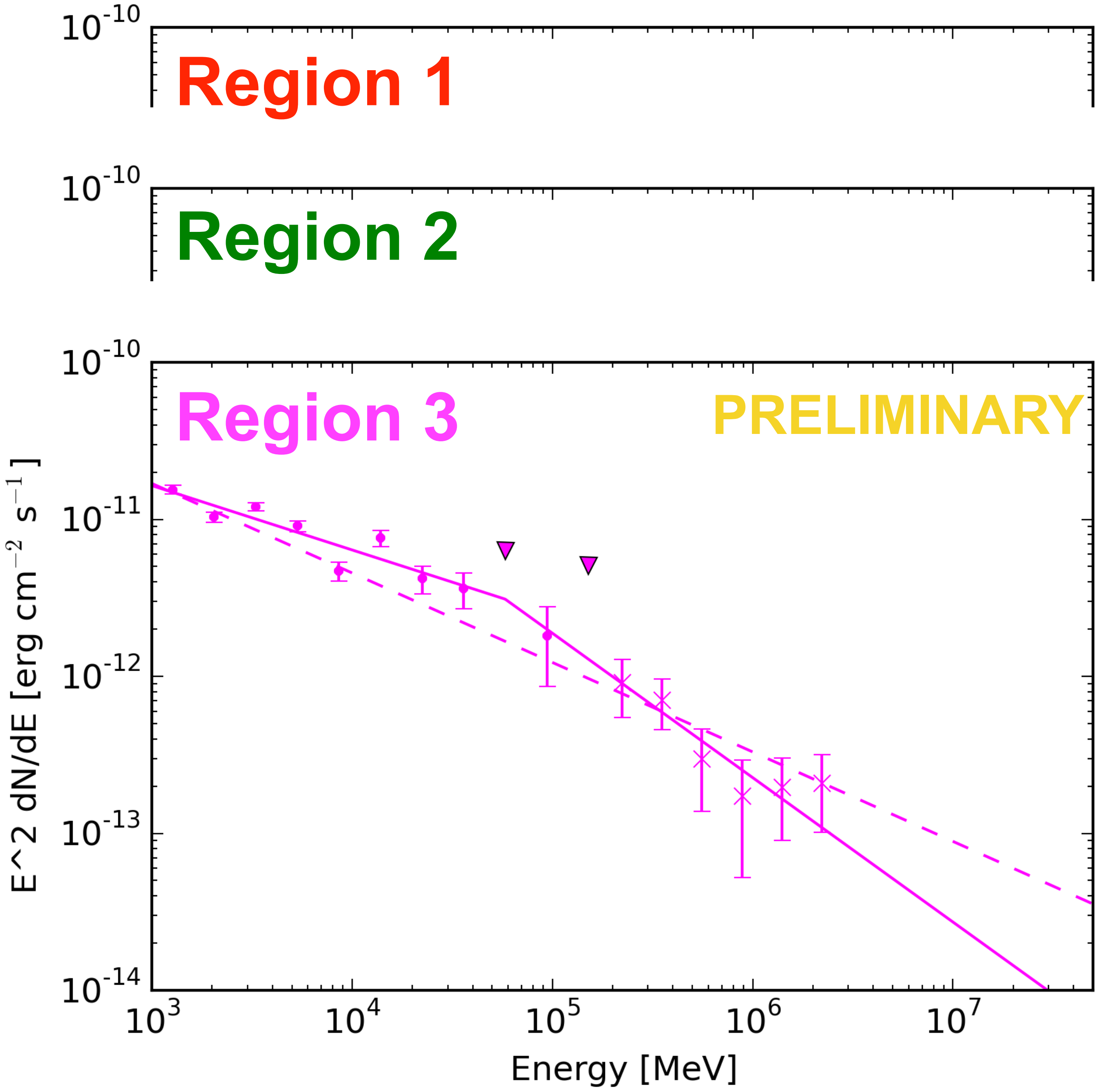

Exploring 4 Distinct Regions

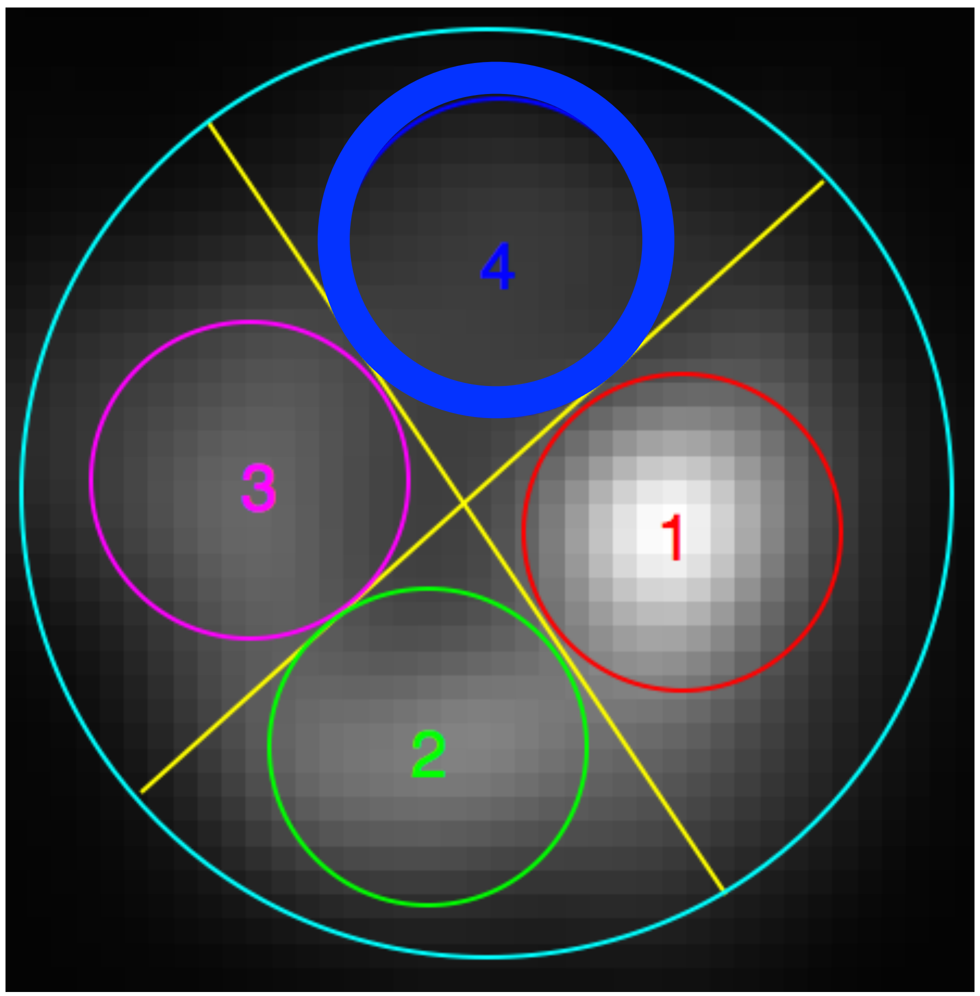

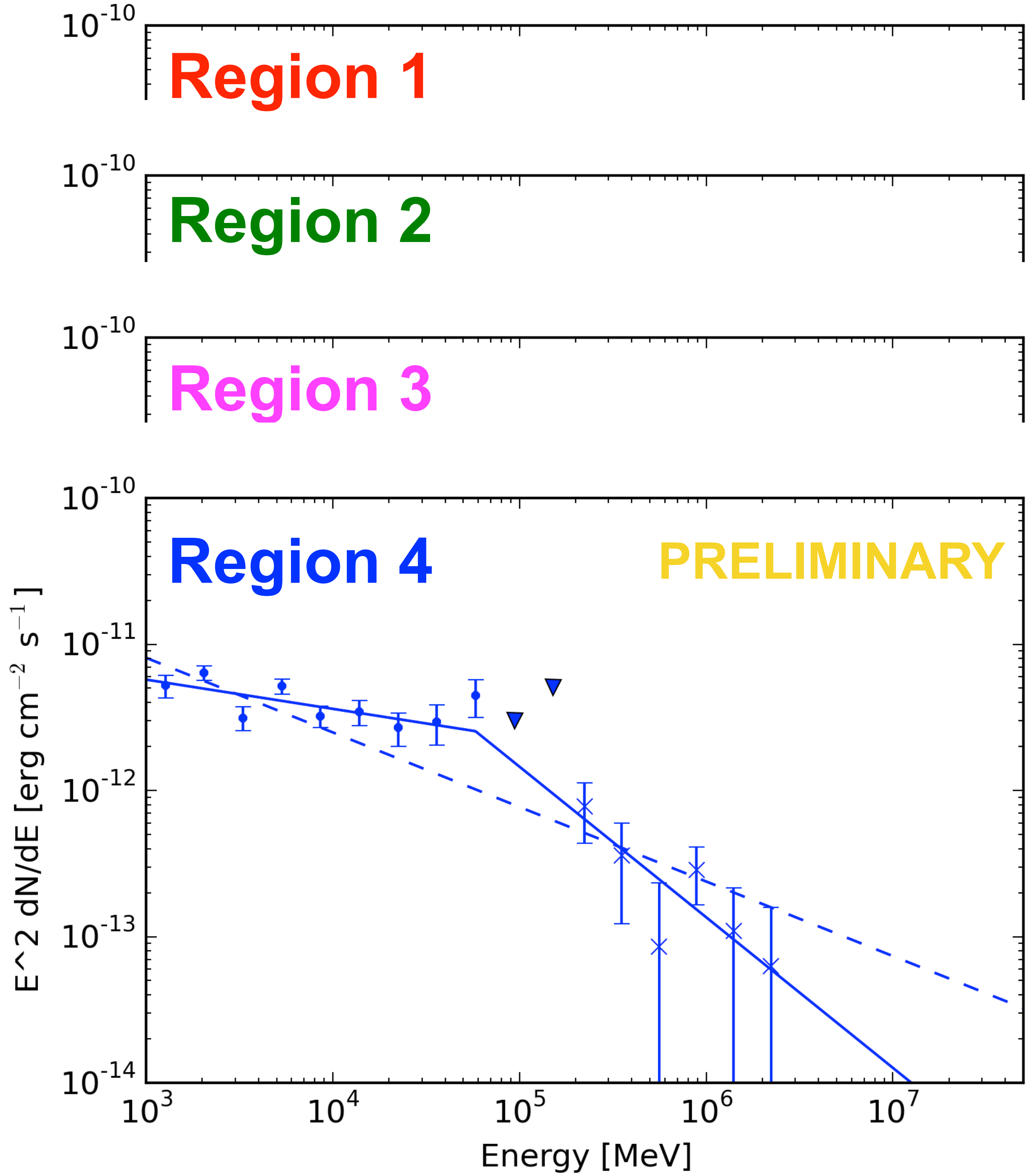

Exploring 4 Distinct Regions

- No clear differences in spectral shape for distinct emission regions (e.g. dense cloud in region 1 vs. fast atomic shock in region 4)

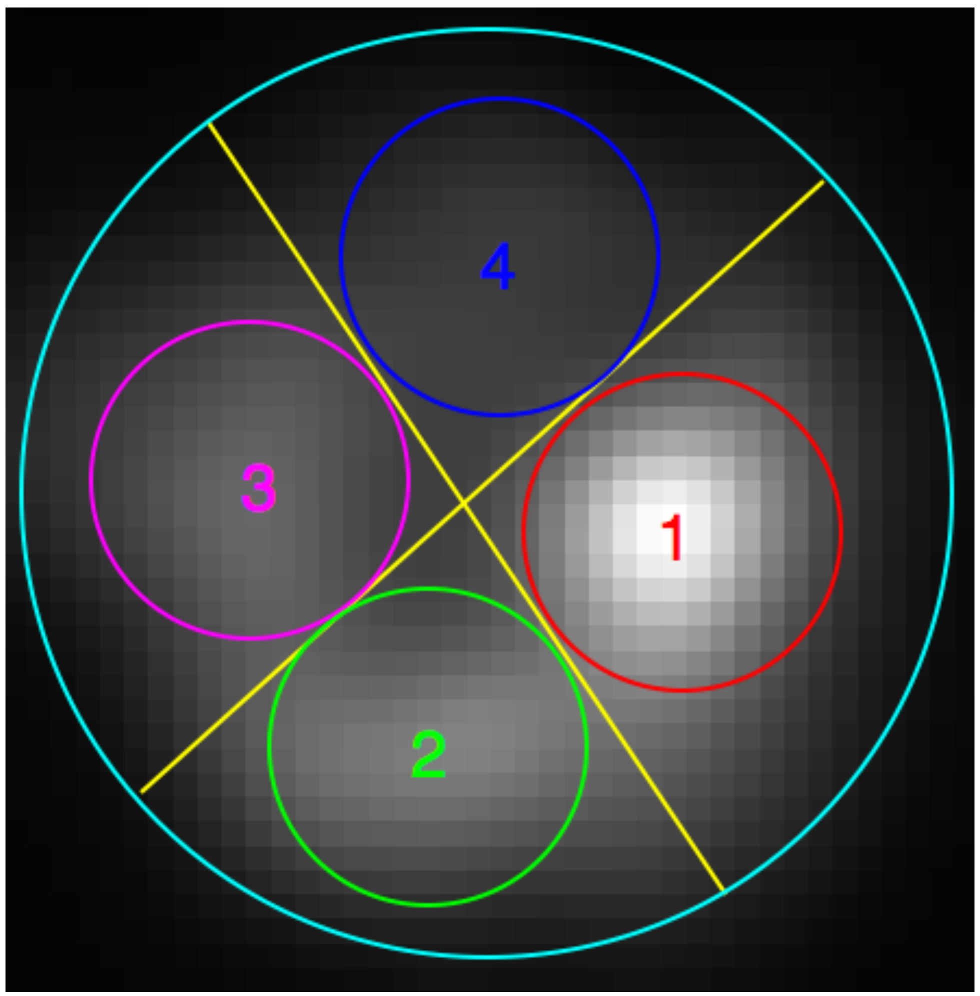

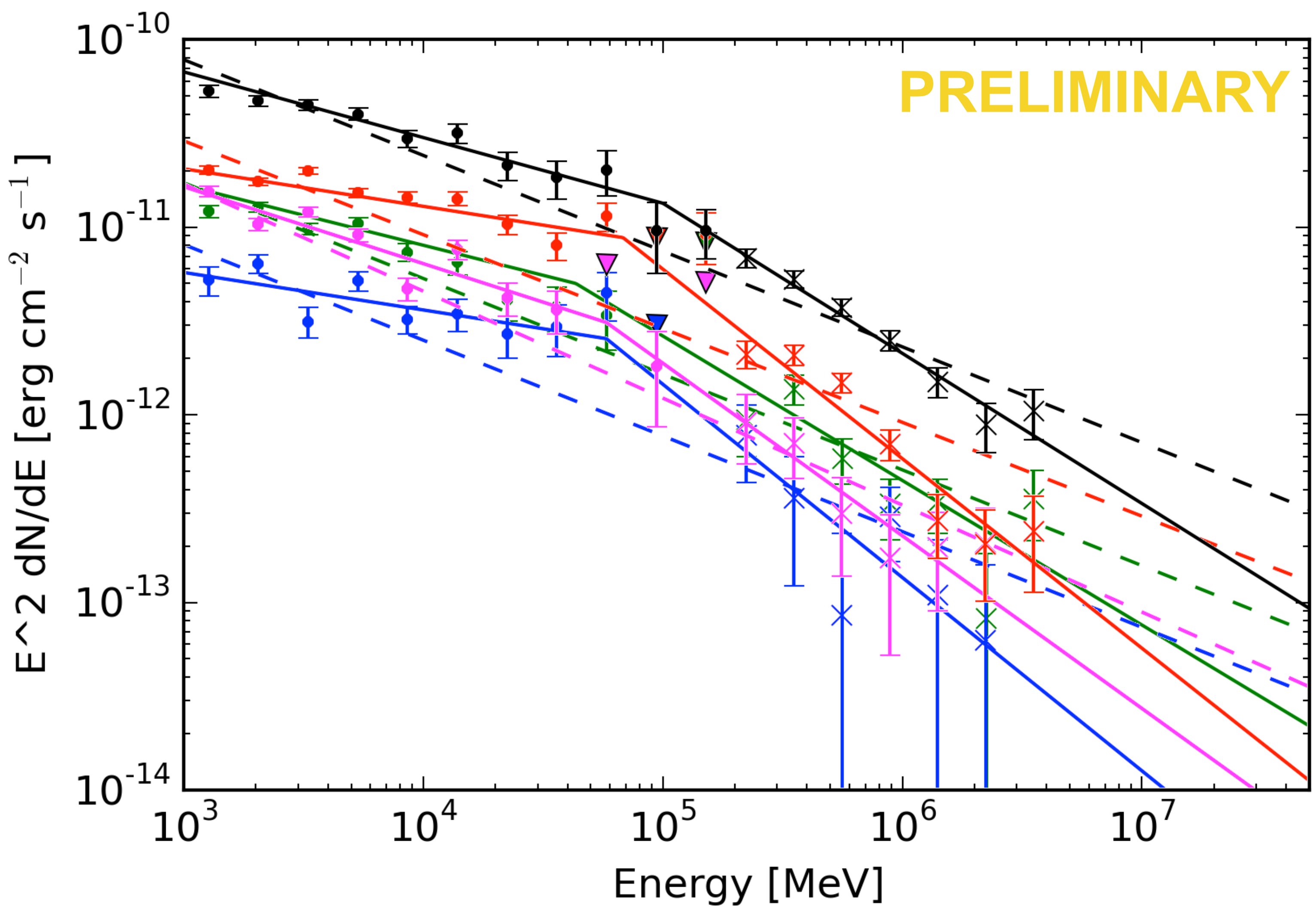

Note: Uncertainties in the absolute flux calibration between Fermi LAT and VERITAS are NOT considered here

Broken PL fits for all 4 regions:
$\Gamma_1 \sim 2.3$, $\Gamma_2 \sim 2.9$, $E_b \sim 60$ GeV

Comparing Regions: GeV vs TeV fluxes

- TeV/GeV integral flux ratios are consistent within errors between all 4 regions, despite ~10x change in brightness

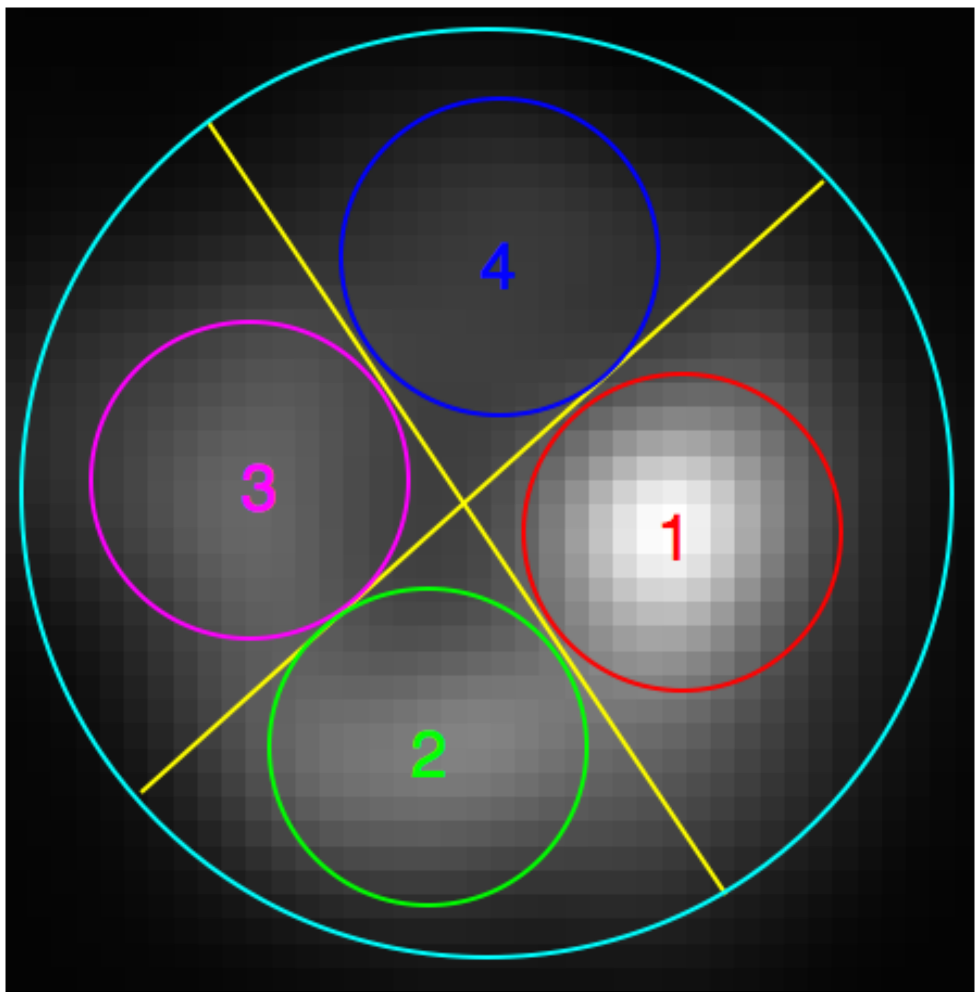

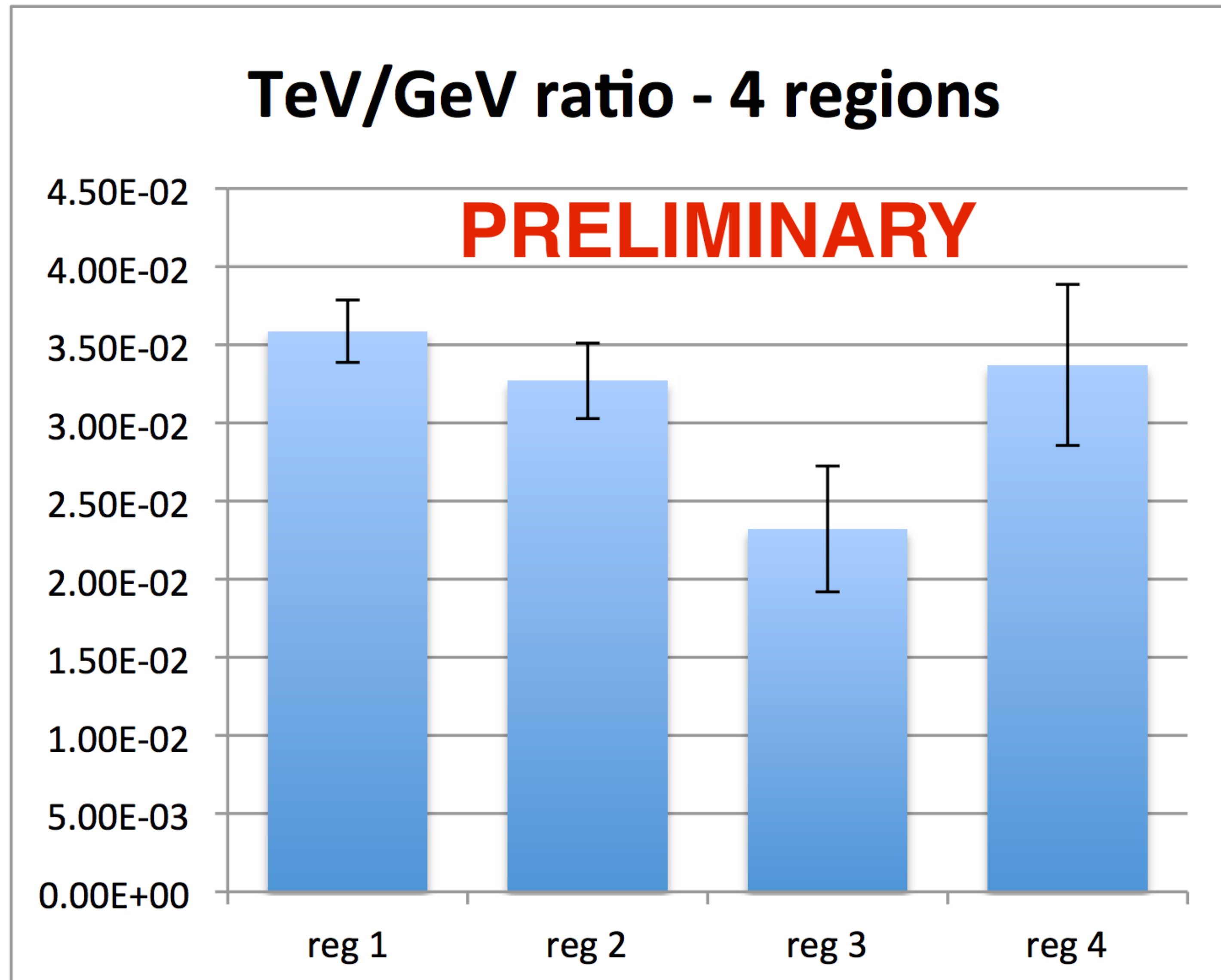

E^2 dN/dE [erg cm^{-2} s^{-1}] flux ratios of the 1-200 GeV and 0.2-6 TeV energy ranges

Comparing Regions: GeV flux vs Gas Mass

- Ratio of flux to gas mass shows significant differences between the dense molecular (1,2,3) and diffuse atomic (4) regions

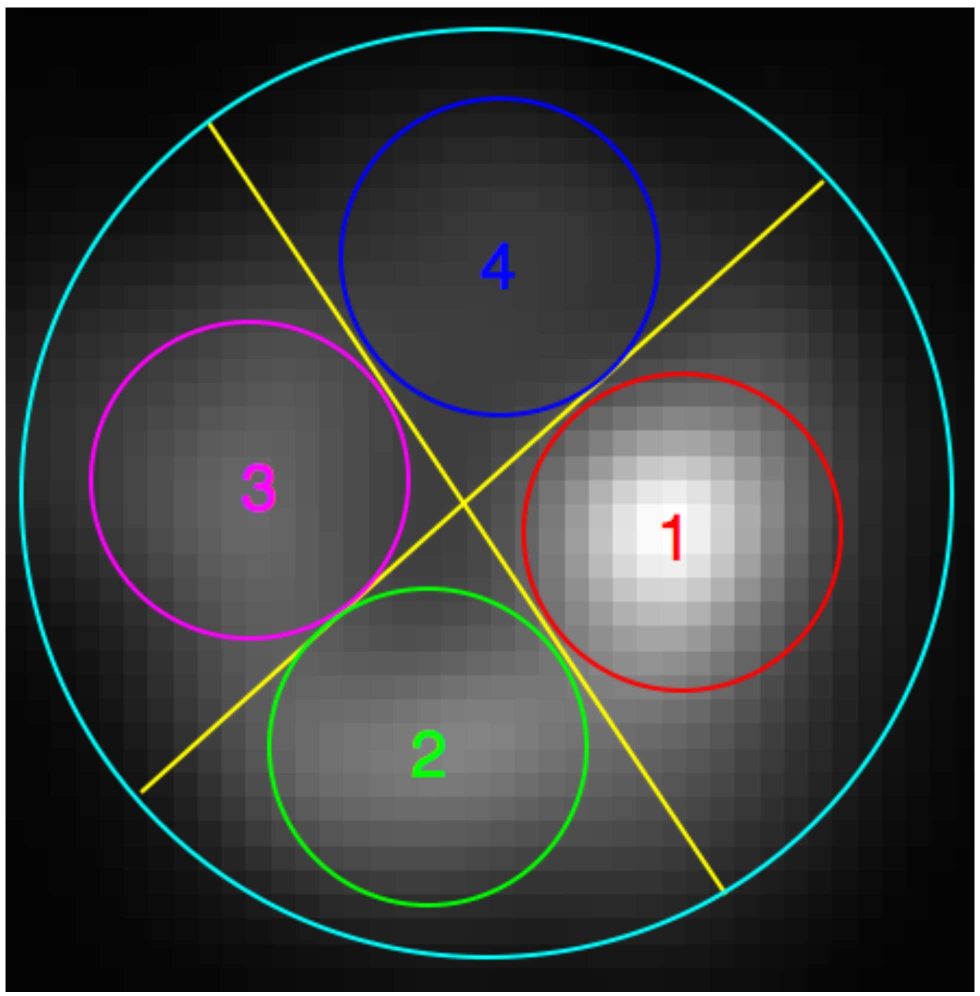

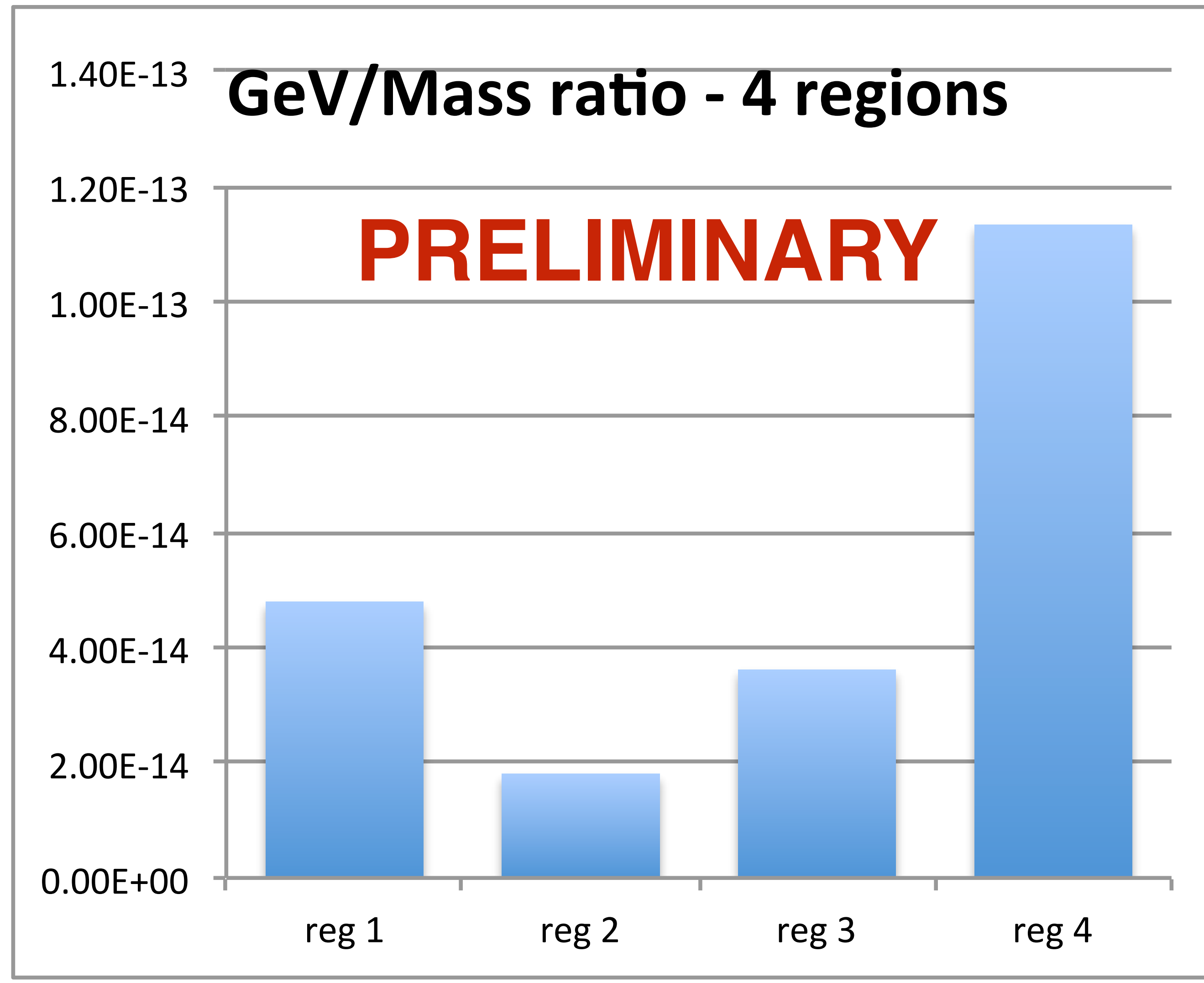

M_γ~2,500 M_{sun} can explain ζ_{CR} ~2×10^{-15} from H_3^+ (Indriolo, et al. 2008)

γ-ray Morphology of IC 443 Resolved

- *Fermi* LAT Pass 8 data resolves γ-ray shell from IC 443 in agreement with deep VERITAS observations
- Able to resolve γ-ray emission zones on ~5 pc scales in IC 443
- GeV/TeV correspondence with shock interaction gas density
- Spectra of all 4 regions show consistency with same broken power law
- *Data are still statistics limited…*

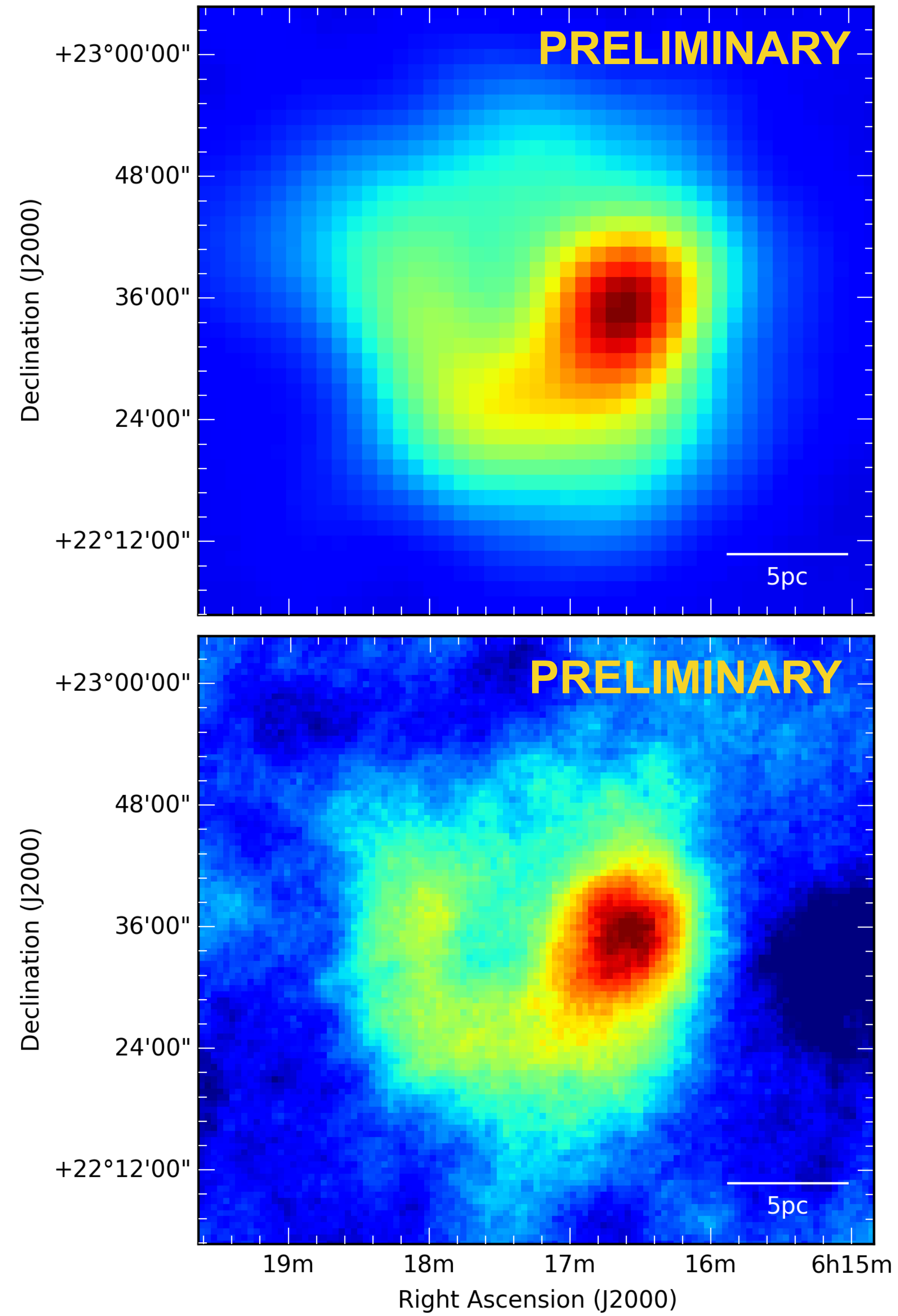

Backup Slides

Energy-Dependent GeV Morphology

***Fermi* LAT** extension fit in 6 distinct energy bins from 0.3-1,000 GeV

Gaussian R_{68} and 1σ localization

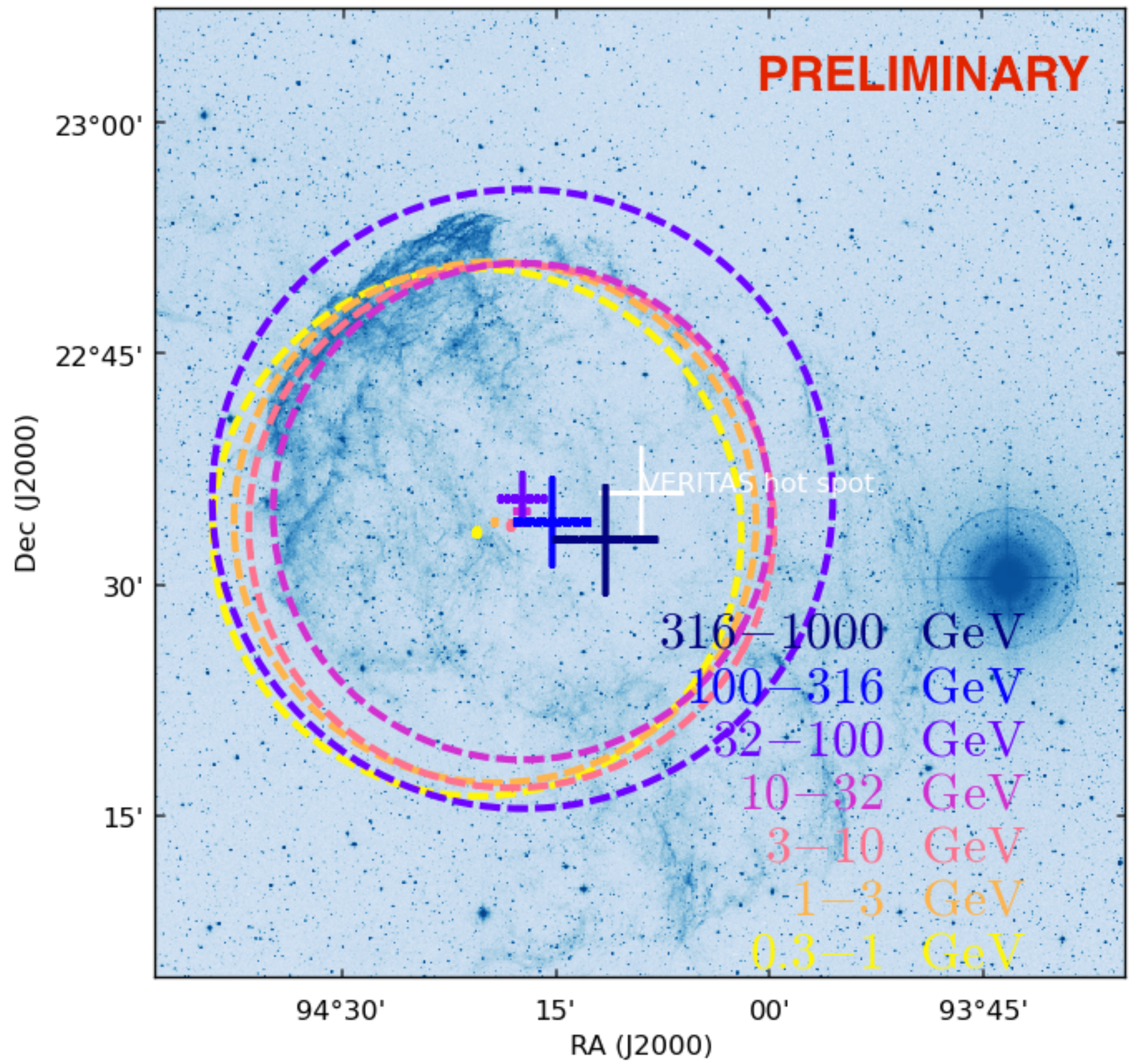

Extension significance

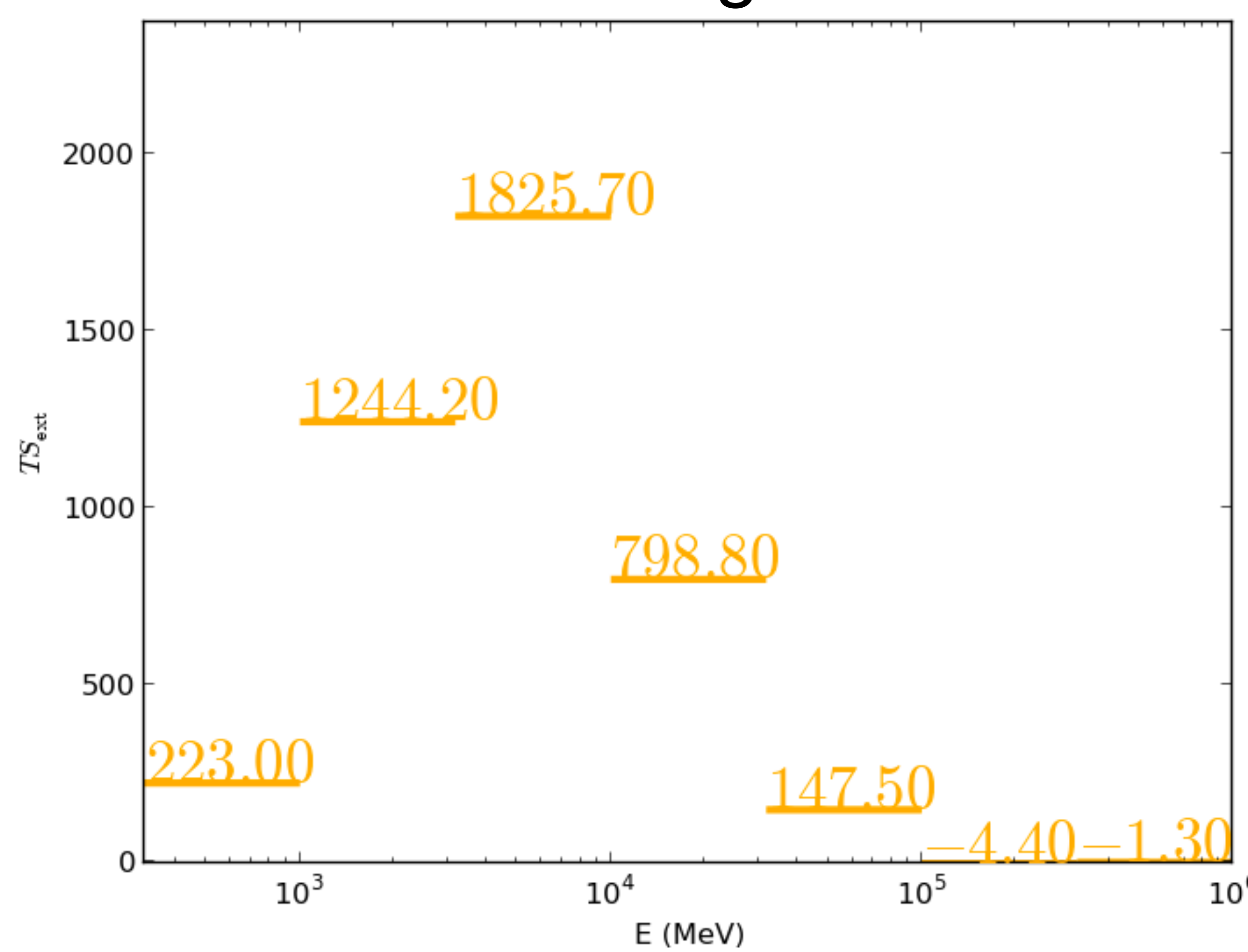

Two nearby molecular clouds

- Foreground molecular cloud cuts across SNR.

  RGB image shows v_{LSR} = -2,-4,-6 km/s against Radio contours

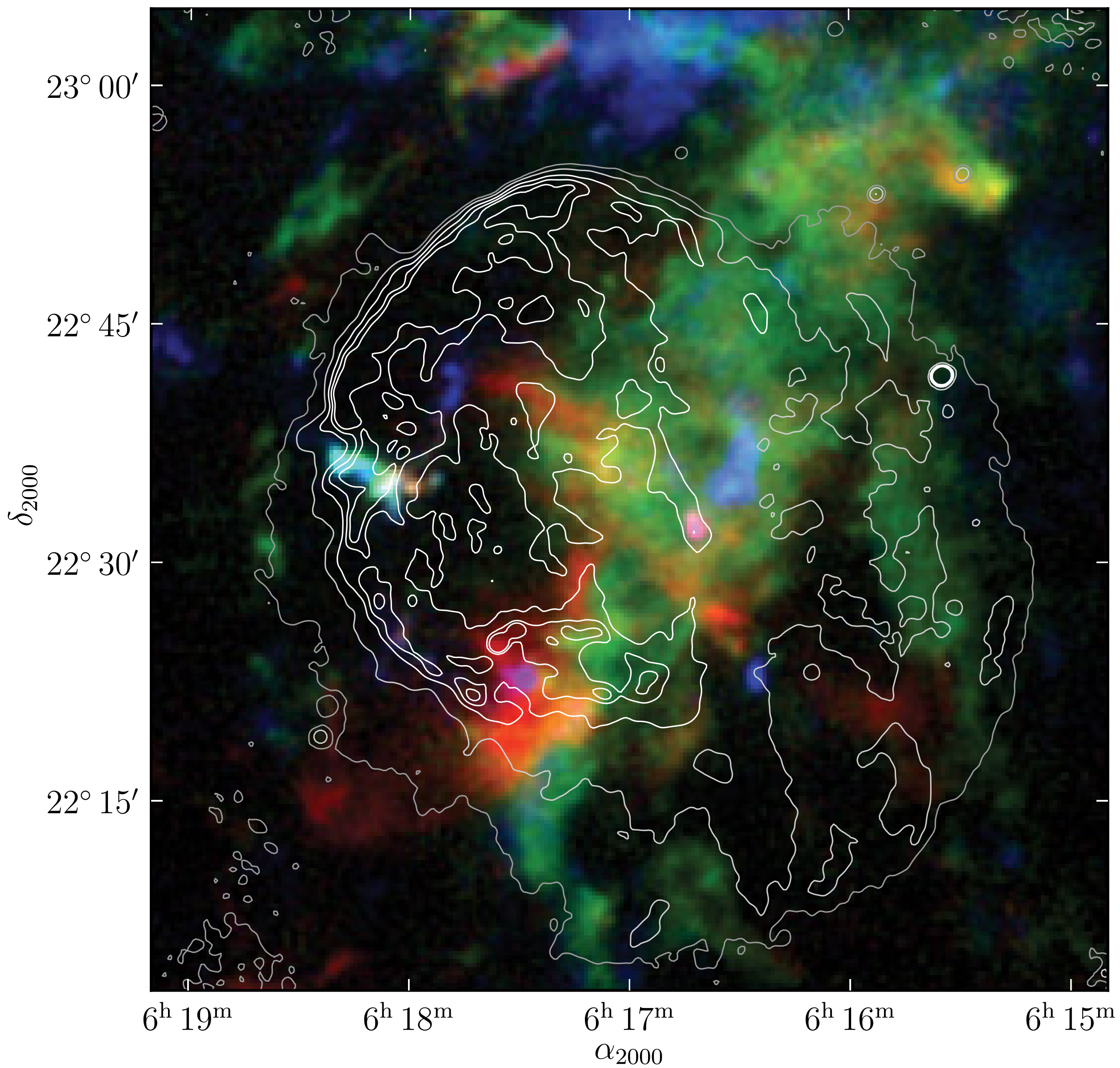

Figures from Lee+ 2008

- +5 km/s cloud ends at TeV peak

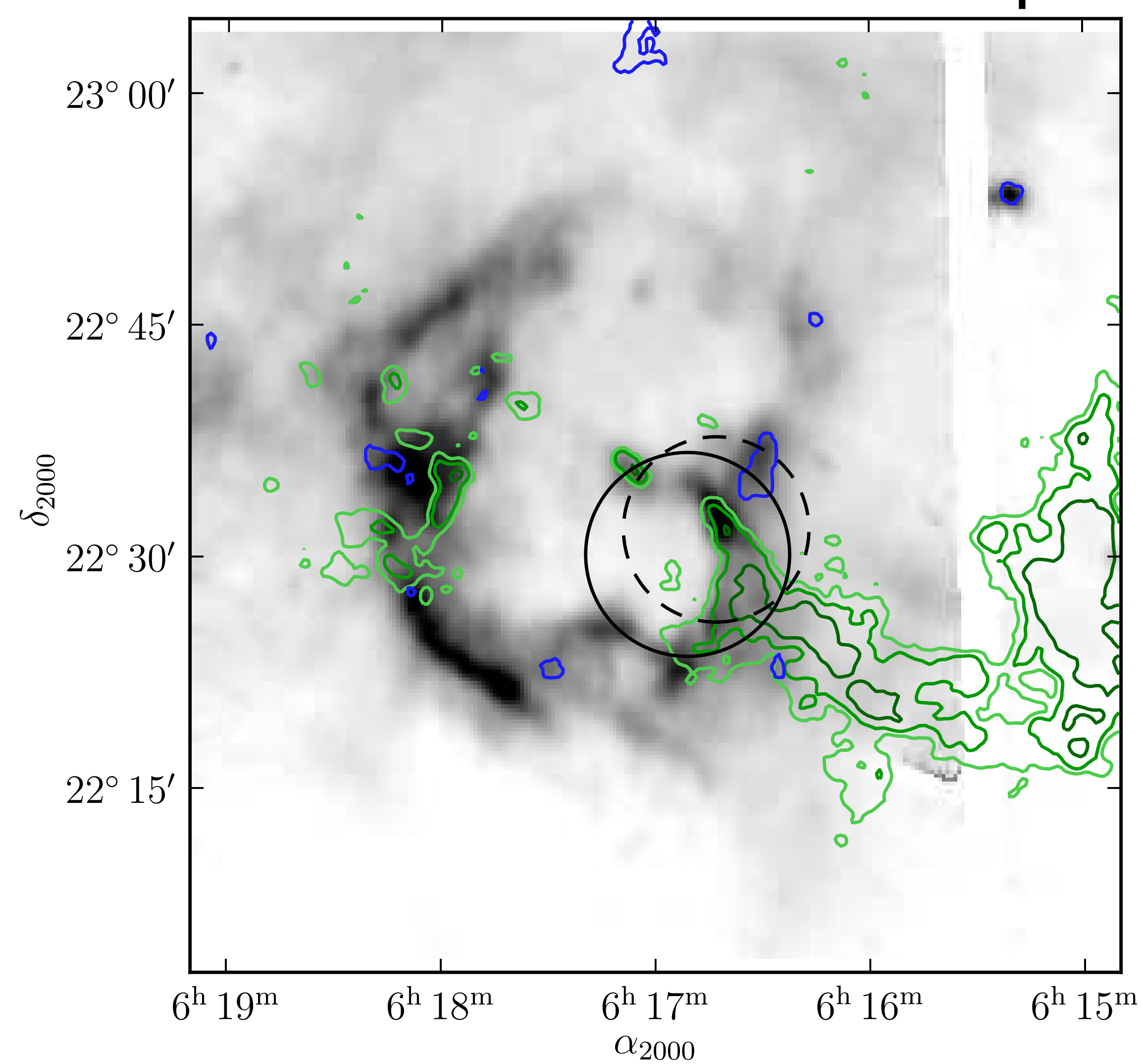

Figure 15. Far-IR 90 μm image taken with the *AKARI* satellite shown in gray scale. The green contours show the distribution of +5 km s^{-1} clouds (the gray scale in Figure 9). The blue contours show locations of SCs. The solid and dashed circles represent the location of γ-ray sources detected by MAGIC and VERITAS, respectively.

Image Restoration Technique

- **Richardson-Lucy Deconvolution Algorithm**
  - When we observe an event at position x
    - P(x:ξ): probability that it came from a "true" position ξ due to instrument response

$$\psi^{r+1}(\xi) = \int \tilde{\phi}(x) \frac{\psi^{r}(\xi) P(x:\xi)}{\int P(x:\zeta)\psi^{r}(\zeta)d\zeta} dx$$

Lucy 1974
Richardson 1974

    - Generalization to Event-by-event $P_k(x:\xi)$

$$\psi^{r+1}(\xi) = \frac{1}{N} \psi^{r}(\xi) \sum_{k=1}^{N} \frac{P_k(x_k:\xi)}{\int P_k(x_k:\zeta)\psi^{r}(\zeta)d\zeta}$$

      - Can be used for event-by-event data with varying PSF.
    - No energy spectrum assumption necessary
  - Point sources can be incorporated using dual-channel method

$$\psi = \psi_{\text{point}} + \psi_{\text{extended}}$$

Hook&Lucy 1994

Wavelet Denoising

- **Minimize the effect of Poisson noise**
  - » **Wavelet filtering technique**

Starck&Murtagh 1994

ϕ: observed image

$R^n = \phi - \phi^n$, $\phi' = R'^n + \phi^n$

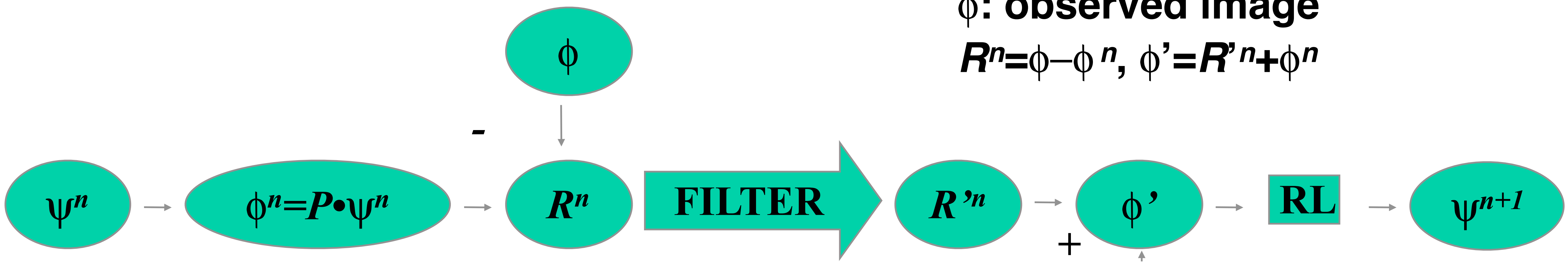

Wavelet decomposition

$$\psi = \sum_{j=0}^{n} w_j + c_n$$

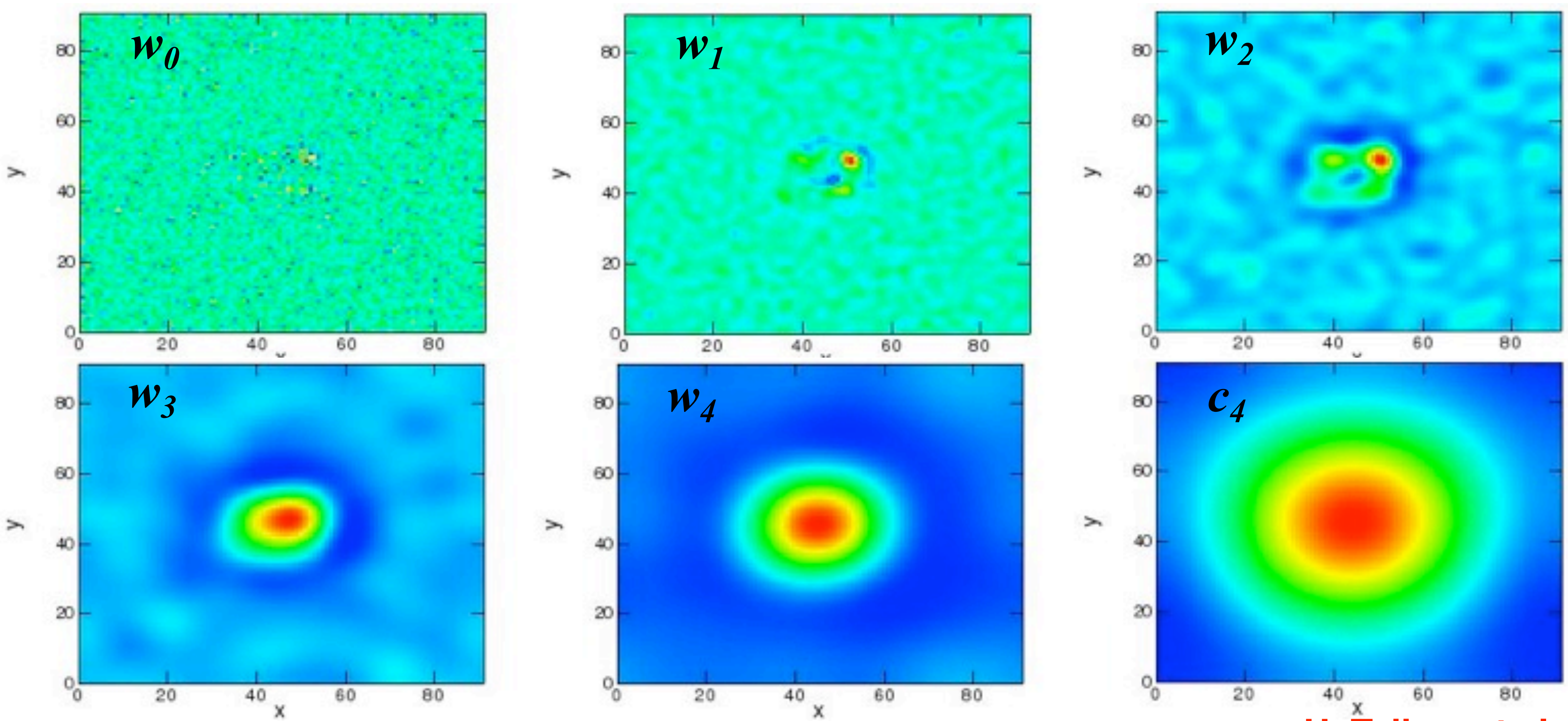

Tajima, et al. (2007) proc. from 1st Fermi Symposium; arXiv:0705.1362